# Challenge Journal of CONCRETE RESEARCH LETTERS

Vol.11 No.3 (2020)

acoustic emission artificial neural network compressive strength concrete cracking curing ductility corrosion durability energy absorption ferrocement flaky aggregate fly ash fracture mortar palm oil fuel ash reinforced concrete scrap self-compacting concrete silica fume strengthening superplasticizer tensile strength waste disposal water absorption



### **EDITOR IN CHIEF**

Prof. Dr. Mohamed Abdelkader ISMAIL

Miami College of Henan University, China

### **EDITORIAL BOARD**

Prof. Dr. Abdullah SAAND

Prof. Dr. Alexander-Dimitrios George TSONOS

Prof. Dr. Ashraf Ragab MOHAMED

Prof. Dr. Ayman NASSIF

Prof. Dr. Gamal Elsayed ABDELAZIZ

Prof. Dr. Han Seung LEE

Prof. Dr. Zubair AHMED

Prof. Dr. Jiwei CAI

Assoc. Prof. Dr. Meral OLTULU

Dr. Aamer Rafique BHUTTA

Dr. Khairunisa MUTHUSAMY

Dr. Mahmoud SAYED AHMED

Dr. Jitendra Kumar SINGH

Dr. Saleh Omar BAMAGA

Dr. Türkay KOTAN

Quaid-e-Awam University of Engineering, Pakistan

Aristotle University of Thessaloniki, Greece

Alexandria University, Egypt

University of Portsmouth, United Kingdom

Benha University, Egypt

Hanyang University, Republic of Korea

Mehran University, Pakistan

Henan University, China

Atatürk University, Turkey

Universiti Teknologi Malaysia, Malaysia

Universiti Malaysia Pahang, Malaysia

Ryerson University, Canada

Hanyang University, Republic of Korea

University of Bisha, Saudi Arabia

Erzurum Technical University, Turkey

E-mail: cjcrl@challengejournal.com

Web page: cjcrl.challengejournal.com

TULPAR Academic Publishing www.tulparpublishing.com





### **CONTENTS**

Research Articles	
Effect of catalysts amount on mechanical properties of polymer concrete  Ferit Cakir, Pinar Yildirim, Mustafa Gündoğdu	46-52
Analytical and experimental study on shear performance of RCC beam elements reinforced with PSWC rebars: a comparative study  Shoib Bashir Wani, Sarvat Gull, Ishfaq Amin, Ayaz Mohmood	53-68
Fracture patterns and mechanical properties of GFRP bars as internal reinforcement in concrete structures  Mehmet Canbaz, Uğur Albayrak	69-74
Comparative study of optimum cost design of reinforced concrete retaining wall via metaheuristics  Aylin Ece Kayabekir, Melda Yücel, Gebrail Bekdaş, Sinan Melih Nigdeli	75-81





### Research Article

# Effect of catalysts amount on mechanical properties of polymer concrete

Ferit Cakir a,\* , Pinar Yildirim a , Mustafa Gündoğdu b

### **ABSTRACT**

Polymer materials are used in different engineering applications because of their excellent engineering properties. The use of these materials in different engineering fields has increased in recent years. It is predicted that polymer materials will be one of the most remarkable and popular engineering materials in the near future because of their unique properties. This paper focuses on Methyl Ethyl Ketone Peroxide (MEKP), which is one of the main catalysts and investigate its effect on the mechanical properties of Polymer Concrete (PC). The main aims of the study are to understand the mechanical properties of the polymer concrete including different amount of MEKP and to investigate the influence of MEKP on the mechanical characterizations of the PCs. For this purpose, five different samples containing 0.15% (Mixture-1), 0.25% (Mixture-2), 0.35% (Mixture-3), 0.45% (Mixture-4) and 0.55% (Mixture-5) MEKP of the total weight were prepared and some experimental studies were performed on the prepared mixtures. The obtained strength values were discussed and evaluated effect of MEKP on mechanical properties of PCs.

### ARTICLE INFO

Article history: Received 29 March 2020 Accepted 1 May 2020

Keywords:
Polymer concrete
Methyl ethyl ketone peroxide
Catalyst
Mechanical tests

### 1. Introduction

Polymers are synthetic materials having a chain structure and atomic groups with chemical bonds. These synthetic materials might be categorized into three different groups as natural polymers, synthetic polymers and semi-synthetic polymers (Ozturk, 2013). General properties of polymers such as heat and electricity insulation, and resistance to chemical and environmental effects have put forward the importance of these materials. These materials are of utmost importance for the construction industry too thanks to their low shear resistance, high tensile and compressive strength, effective hardening time, and high surface hardness. High performance structural elements consisting of polymer concrete advanced the studies on the polymer industry.

The use of polymers in structural elements can be grouped into three: a combination of polymer and Portland cement concretes (PCCs), polymer impregnated concretes (PICs), and synthetic resin concretes (polymer

concretes, PCs). In the production to PCCs, the polymer is directly added to the concrete by consideration of the weight of cement. The permeability and compressive strength increase for this type of concrete, because of the decrease in the void ratio. PCCs are generally used in construction elements that necessitate repairs. On the other hand, PICs are obtained by impregnating the monomer into the hardened concrete. The monomer is provided to fill the voids in the concrete by applying pressure or vacuum. This process is generally applied to the structural elements needing reinforcement. Moreover, PCs is a composite material in which the binder consists of a synthetic polymer. In PCs, cement and water are not used in the production of concrete. Many different studies have been carried out on these three types of concrete. In previous studies, Kukacha (1978) concentrated on PICs. In the study, it was concluded that PICs are beneficiary especially in the strengthening and renovation works for the studies on the use of polymers in structures. In the study, it was concluded that the compressive

<sup>&</sup>lt;sup>a</sup> Department of Civil Engineering, İstanbul Aydın University, 34295 İstanbul, Turkey

<sup>&</sup>lt;sup>b</sup> Mert Casting Industrial Trade Inc., 34775 İstanbul, Turkey

strength significantly increased in PICs. In addition, it was emphasized that wear, chloride, acid, freeze-thaw resistance significantly increased, and water absorption rate decreased by 99% (Kukacha, 1978). In another study, Vipulanandan and Mebarkia (1993) conducted an experimental study on the flexural strength, toughness, and fracture properties of PCs.

In this study, the flexural behavior of the particulate fiber-reinforced polyester composite was investigated by changing the polymer and fiber content. The study used cobalt naphthenate (0.3% resin) and methyl ethyl ketone peroxide (1.5%) as binders. The study concluded that the use of aggregates and fibers treated with silane increased the strength of PCs. In addition to these studies, some studies were conducted on fiber reinforced polymer concretes (FRPCs). For example, Griffits and Ball's (2000) studied flexural strength and fracture toughness values by using different fiber reinforced techniques and silane binders. The study determined that fiber reinforcement and silane binders significantly change the flexural strength. Achek and Aztekin (2011) performed an experimental study on the density and compressive strength of FRPCs. The study determined suitable polyester, hardener and catalyst ratios for FRPCs in the results of the study.

Another issue in polymer concrete is strongly rinse onto the catalyst used in the polymer concrete. Today, Methyl Ethyl Ketone Peroxide (MEKP) is one of the catalysts used in polymer concrete. MEKP is a material, which is active at room temperature for hardening of polyesters. By cross-linking between resin and monomers, the material initiates hardening. MEKP, which is

used as a catalyst in polymer concrete, is generally used in combination with materials such as cobalt, which have accelerating effect.

This study focuses on MEKP catalyst and effect of MEKP on mechanical properties of PCs. The main purpose of this study is (1) to understand the mechanical properties of the polymer concrete including different amount of MEKP and (2) to investigate the influence of MEKP on the mechanical characterizations of the polymer concrete.

### 2. Materials and Methods

The experimental program in this study was realized at Civil Engineering Laboratories at İstanbul Aydın University (IAU), with the collaboration of Mert Döküm Construction and Trade Inc. A part of the samples was supplied by Mert Döküm and the experimental tests were performed at Structural Materials and Structural Mechanics Laboratory and at IAU.

Polymer concrete consists of aggregates with different granulometry, binder, hardener and accelerator. In this study, size of 0.3–1 mm, 1–2 mm, 2–3 mm and 3–5 mm silica sands, polyester resin, MEKP and cobalt were used as an aggregate mixture, binder, hardener and accelerator, respectively. The aggregates used in the study were supplied by Yelten Mining and Kumsan Döküm from Kirklareli and İstanbul, Turkey. All aggregates were washed with clear water to remove any contaminated materials and dried before using. Its chemical composition is given in Table 1.

Chemicals		Aggre	egates	
Chemicais	0.3-1 mm	1-2 mm	2-3 mm	3-5 mm
MgO	0.10	0.06	0.06	0.06
$Al_2O_3$	0.245	1.86	1.86	1.86
SiO <sub>2</sub>	98.86	94.15	94.15	94.15
CaO	0.01	0.39	0.39	0.39
$Fe_2O_3$	0.148	0.46	0.46	0.46
SO <sub>3</sub>	-	0.10	0.10	0.10
K <sub>2</sub> O	0.03	1.56	1.56	1.56
Na <sub>2</sub> O	0.02	1.12	1.12	1.12
Ignition Loss	0.24	0.30	0.30	0.30

**Table 1.** Chemical composition of the aggregates.

In this study, an experimental study was conducted in order to investigate the effects of MEKP on the flexural and compressive strength of PC at İstanbul Aydın University, Civil Engineering Department Laboratory with support from Mert Dokum Construction Industry and Trade Inc. For this purpose, five different samples containing 0.15% (Mixture-1), 0.25% (Mixture-2), 0.35% (Mixture-3), 0.45% (Mixture-4), and 0.55% (Mixture-5) MEKP of the total weight were prepared and compressive and flexural tests were performed on the prepared mixtures. A total of 15 pieces of specimen having

40x40x160 mm prisms and 40x40x40 mm cubes were prepared for each mixture (Fig. 1a). The chemical properties of MEKP used are shown on Table 2.

Before the basic specimens are produced; other variables have been kept constant and specimens have been prepared by using aggregates with different maximum diameters. The most suitable maximum aggregate grain diameter has been determined as 4 mm. Then the method for adding catalyst has been selected. Different methods are used for the addition of catalyst in PC production.

- a) The catalysts are mixed directly into the resin and then mixed with the aggregate,
- b) Addition of the resin after mixing the catalysts with the aggregate,
- c) Addition of catalysts after mixing of aggregates with resin

In this study, the wet mixture was prepared by adding the aggregates with resin. MEKP and the accelerators were added to the wet mixture in the final step. After completion of the mixing process, fresh concrete was cast in steel prism molds gradually (Fig. 1b). In order to obtain full homogeneity and compaction, the fresh concrete was carefully compacted with shaking table during 120 second (Fig. 1c). The specimens were kept in the molds up to curing. After remolding, the specimens were stored at  $20 \pm 2$  °C in the laboratory for up to 7 days (Fig. 2). In the scope of the study, five different mixtures containing 0.15% (Mixture-1), 0.25% (Mixture-2), 0.35% (Mixture-3), 0.45% (Mixture-4) and 0.55% (Mixture-5) MEKP (the total weight of PC) were prepared. For each mixture, three samples were prepared, and the experimental studies were conducted by using these samples.

**Table 2.** Technical properties of MEKP.

Properties	Values
Flash Point	> 80 °C
Density	1,12 g/cm <sup>3</sup> (20°C)
Viscosity	19 mPa.s (20°C)
Self-Accelerating Decomposition Temperature (SADT)	>= 60°C
Active oxygen	9.7%
Free Hydrogen Peroxide Content	2.2%
Water Content	2.0%
рН	5.2
Critical Temperature (SADT)	65°C
Gel Time	18 min
Peak Time	48 min
Exothermic Temperature	106°C





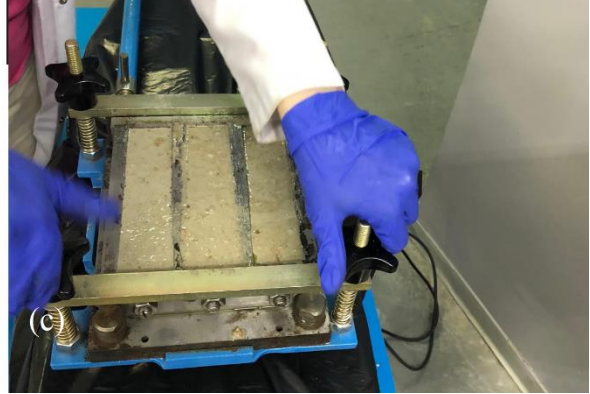


**Fig. 1.** Preparation of the PCs: (a) 40x40x160 mm steel molds; (b) cast in steel prism molds; (c) compaction with shaking table.



Fig. 2. Test samples.

### 3. Experimental Studies

Within the scope of the study, the experimental studies were carried out in two basic steps. The first step was to determine the initial and the final setting times, and the second step was to determine the mechanical properties of the materials with the mechanical tests. The initial and final setting times of the mixtures were determined by using VICAT apparatus.

After remolding, the samples were stored at 20±2°C in the laboratory for up to 7 days. In the second step of the experimental studies, it was intended to investigate the mechanical properties of the samples. In the tests,

the densities of the samples were determined before the mechanical tests (Table 4). Then, three-point bending tests and compression tests were conducted the hardened specimens. All tests were carried out according to relevant Turkish and ASTM specifications at the laboratories of the Department of Civil Engineering at İstanbul Aydın University (IAU). The tests were conducted on three specimens at 7 days and all tests were performed on a U-Test hydraulic test machine (Fig. 3).

### 4. Results and Discussions

The use of polymer materials in different engineering fields is increasing and polymer materials are used effectively in different engineering applications. Thanks to its unique properties, these materials are considered to be among the most remarkable and popular engineering materials in the near future. This paper focuses on Methyl Ethyl Ketone Peroxide (MEKP), which is one of the main catalysts and investigate its effect on the mechanical properties of Polymer Concrete (PC).

The initial setting time and final setting time of the PCs is very short compared to conventional cement concretes. Therefore, in experimental studies, in the first step, the study concentrated on the initial and final setting times of the mixtures. Table 3 shows the initial and final setting times based on the amount of MEKP used. When the initial setting and final setting times were examined, it was determined that the Mixture-4 (0.45% MEKP) reached its strength in the shortest time and the Mixture-1 (0.15% MEKP) reached its strength in the latest time.

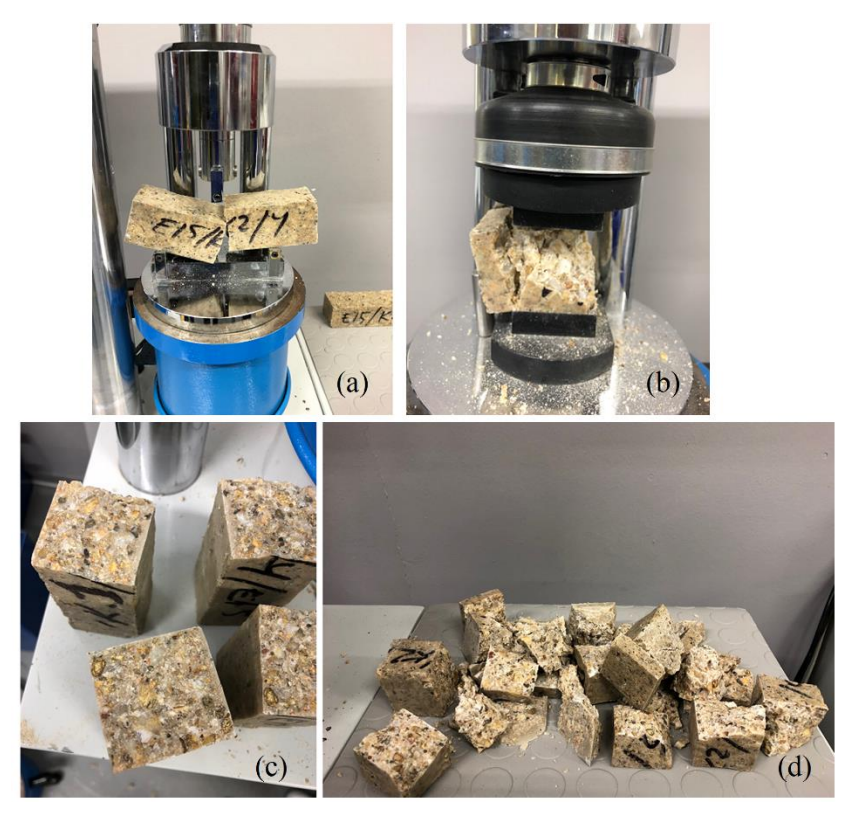


**Fig. 3.** Experimental Studies: (a) three-point bending tests; (b) compression tests; (c) crack pattern after the three-point bending tests; (d) failure mechanisms after the compression tests.

Samples	Initial Setting Time (sec)	Final Setting Time (sec)
Mixture-1	240	1080
Mixture-2	220	840
Mixture-3	210	755

180

200

**Table 3.** Initial and final setting times of the samples.

In the second step of the experimental studies, the mechanical tests were conducted. The loading rates were 0.05 kN per second and 2.4 kN per second for the three-point bending tests and compression tests, respectively. In the mechanical tests, the samples were loaded with this velocity until they collapse. Table 4 provides a summary of the mechanical test results.

Mixture-4

Mixture-5

It was found that the amounts of the MEKP played an important role in the mechanical properties of PCs. Sim-

ilarly, Khalid et al. 2015 and Mahdi et al. 2010 emphasized the same issue in the literature. When the mechanical test results were examined, the highest flexural strength was determined in the Mixture-2 and the highest compression strength was determined in the Mixture-1. The lowest flexural strength determined in the Mixture-1 and the lowest compression strength was determined in the Mixture-5. The average values are presented in Fig. 4 for easy evaluation.

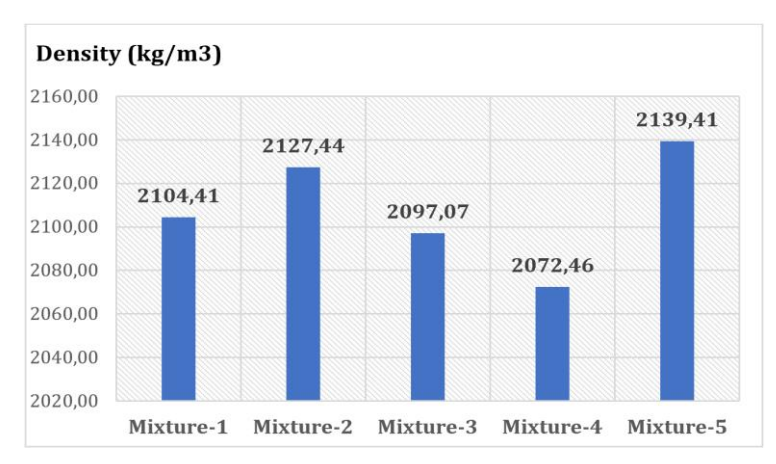
660

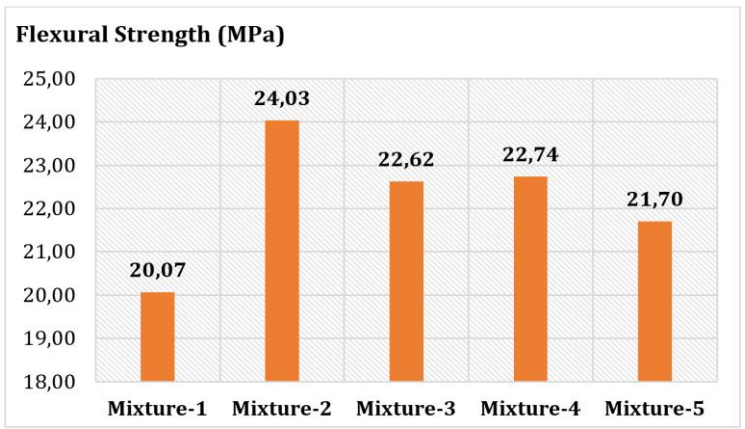
720

Table 4. Mechanical test results.

Samples		Amount of MEKP (%)	Density (kg/m³)	Flexural Strength (MPa)	Compression Strength (MPa)
	1	0.15	2105.98	19.03	109.55
Mixture-1	2	0.15	2104.14	21.05	110.31
	3	0.15	2103.12	20.13	109.96
	Avera	ige	2104.41	20.07	109.94
	1	0.25	2125.98	24.47	107.57
Mixture-2	2	0.25	2119.14	23.53	109.01
	3	0.25	2137.20	24.09	108.26
	Avera	ige	2127.44	24.03	108.28
	1	0.35	2095.98	22.52	108.11
Mixture-3	2	0.35	2104.14	22.73	108.87
	3	0.35	2091.09	22.61	108.46
	Avera	ige	2097.07	22.62	108.48
	1	0.45	2069.98	22.76	103.77
Mixture-4	2	0.45	2074.14	22.71	104.83
	3	0.45	2073.26	22.75	104.33
	Avera	ige	2072.46	22.74	104.31
	1	0.55	2135.98	22.41	103.21
Mixture-5	2	0.55	2144.14	21.02	104.13
	3	0.55	2138.11	21.67	103.64
	Avera	nge	2139.41	21.70	103.66

In the last step, the failure mechanics and crack patterns the samples were examined based on the flexural and compression tests. It was observed that fracture was brittle in all samples as expected. Fig. 5 shows that the failure generally occurred on the aggregate grains. Because of the brittle behavior, compression fractures became sudden and the specimens were separated into many pieces. Therefore, one might conclude that these PC specimens do not either have plastic deformation capacity or have low plastic deformation capacity.





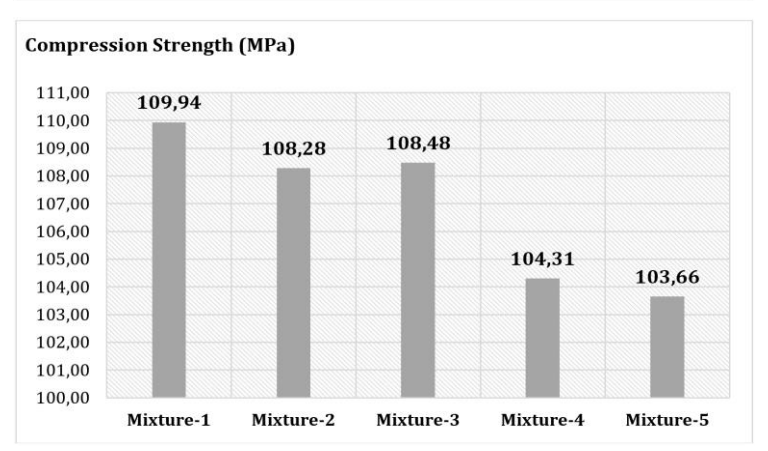


Fig. 4. Average values of the mechanical test results.



Fig. 5. Failure surface of the sample.

### 5. Conclusions

This study investigates the mechanical properties of the PCs including different amount of MEKP evaluates the influence of MEKP on the mechanical characterizations of the PCs. The main purpose of this study is (1) to understand the mechanical properties of the polymer concrete including different amount of MEKP and (2) to investigate the influence of MEKP on the mechanical characterizations of the polymer concrete. For this purpose, five different samples containing 0.15% (Mixture-1), 0.25% (Mixture-2), 0.35% (Mixture-3), 0.45% (Mixture-4) and 0.55% (Mixture-5) MEKP of the total weight were prepared and compressive and flexural tests were performed on the prepared mixtures. A total of 15 pieces of specimen having 40x40x160 mm in dimension were

produced for each mixture. The results of the experimental samples were examined comparatively, and the main results were listed below.

- The mechanical tests show that the flexural strength of Mixture-2 is better than the other mixtures. It was observed that the flexural strengths decreased in Mixture-3, Mixture-4 and Mixture-5. The lowest value of the flexural strength were determined in Mixture-1.
- Considering the compression strengths of the samples, Mixture-1 has the highest value in all respects compared to other mixtures. It was observed that compressive strengths decreased while MEKP amount increased. It was further determined that the compressive strengths, which are almost same in the Mixture-1, Mixture-2 and Mixture-3, however, the compressive strength of Mixture-4 and Mixture-5 decreased relatively.
- In the experimental tests, brittle fractures were observed in all specimens. As a result of the compression test, the specimens were broken into small pieces. Therefore, it was determined that these PC specimens either do not have plastic deformation capacity or have low plastic deformation capacity. Since all of the specimens have a brittle fracture, it can be concluded that the plastic deformation capacity is irrelevant of the amount of MEKP.
- In case of was prevented fracture of brittle, due to the advantages such as short hardening time, high flexural and compressive strength; polymer concrete's; drainage channels, manholes, bridge beams at flexural effect and bridge legs etc. are widely be used in prefabricated building elements. Therefore, the number of experimental studies in this area is encouraged.
- The amounts of the MEKP do not affect the crack patterns and failure modes of the samples.

### **Acknowledgements**

The authors would like to thank Associate Professor Cem Aydemir who is in charge of Civil Engineering Laboratories at İstanbul Aydın University for his valuable contributions. The authors would like also to thank İsmail Yüksel who is Construction Technician at İstanbul Aydın University and Mert Dokum Construction Industry and Trade Inc. for their continuous support during the study.

### **Publication Note**

This research has previously been presented during the session of 'Special Concretes" of the 10<sup>th</sup> International Concrete Congress held in Bursa, Turkey, on May 2-4, 2019. Extended version of the research has been submitted to Challenge Journal of Concrete Research Letters and has been peer-reviewed prior to the publication.

### REFERENCES

- Ateş E, Aztekin K (2011). Density and compression strength properties of particulated and fiber reinforced polymer composites. *Journal of the Faculty of Engineering and Architecture of Gazi University*, 26(2), 479–486
- Griffits R, Ball A (2000). An assessment of the properties and degradation behaviour of glass-fibre reinforced polyester polymer concrete. *Composites Science and Technology*, 60, 2747–2753.
- Haddad H, Al Kobaisi M (2013). Influence of moisture content on the thermal and mechanical properties and curing behavior of polymeric matrix and polymer concrete composite. *Materials and Design*, 49, 850–856.
- Khalid NHA, Hussin MW, Ismail M, Basar N, Ismail MA, Lee HS, Mohamed A (2015). Evaluation of effectiveness of methyl methacrylate as retarder additive in polymer concrete. *Construction and Building Materials*, 93, 449–456.
- Kukacha LE (1978). Concrete Polymer Materials, Production Methods and Applications. Prepared for presentation at Word of Concrete Symposium, "Polymers in Concrete", January 13, 1978.
- Mahdi F, Abbas H, Khan AA (2010). Strength characteristics of polymer mortar and concrete using different compositions of resins derived from post-consumer PET bottles. *Construction and Building Materials*. 24. 25–36.
- Ozturk M (2013). Some Physical and Mechanical Properties of Polymer-Modified Lightweight Concrete. *M.Sc thesis*, Karadeniz Technical University, Turkey.
- Vipulanandan C, Mebarkia S (1993). Flexural strength, toughness, and fracture properties of polyester composites. *Journal of Applied Polymer Science*, 50(7), 1159-1168.



### Research Article

# Analytical and experimental study on shear performance of RCC beam elements reinforced with PSWC rebars: a comparative study

Shoib Bashir Wani <sup>a</sup> , Sarvat Gull <sup>b,\*</sup> , Ishfaq Amin <sup>c</sup> , Ayaz Mohmood <sup>b</sup>

- <sup>a</sup> Department of Civil Engineering, B. S. Abdur Rahman University, Vandalur 600048, India
- <sup>b</sup> Department of Civil Engineering, National Institute of Technology, Hazratbal, Srinagar 190006, India
- <sup>c</sup> Department of Civil Engineering, Maharshi Dayanand University, Rohtak, Haryana 124001, India

### **ABSTRACT**

Early distress in RCC (Reinforced Cement Concrete) structures in the recent times poses a major problem for the construction industry. It is found that in most of cases, distresses in reinforced concrete structures are caused by corrosion of rebar embedded in the concrete. The HYSD (High Yield Strength Deformed) rebars which are used to offer excellent strength properties is detrimental to durability due to action of ribs as stress concentrators. Nowadays, concept of PSWC rebars (plain surface with wave type configuration rebars, formerly known as C-bars/mild steel rebar with curvy profile) is emerging to have a compromise between strength and durability. This investigation assesses the flexural behaviour of RCC elements reinforced with PSWC rebars. The flexural performance of RC beams of size 1000mm x 150mm x 150mm reinforced with PSWC rebars at 4mm and 6mm deformation level was studied by conducting test as per IS 516-1959 under four point loading. The performance of PSWC bar reinforced elements are compared with beams reinforced with mild steel rebars, HYSD rebars with spiral and diamond rib configuration to assess the viability of PSWC rebars to replace conventional reinforcement. The test results are validated by numerical analysis with the help of ANSYS software. Totally 15 beams are subjected to flexure test and the performance evaluators are first crack load, deflection at first crack load, ultimate load carrying capacity, deflection at ultimate load, loaddeflection behaviour, load-strain behaviour and failure pattern. It is found that PSWC rebars as reinforcement in concrete beams enhanced the ductile behaviour of beams as compared to conventional HYSD and mild steel rebar beams. The energy absorbing capacity has increased significantly for beams reinforced with PSWC rebars when compared with conventional HYSD and mild steel rebar beams. The load-deflection behaviour and failure mode of PSWC rebars reinforced concrete beams were found to be similar to that of high yield strength rebars irrespective of deformation level. The analytical investigation from ANSYS software gave good agreement with the experimental results. It is concluded that PSWC bar has the potential to replace conventional HYSD rebar. Further study needs to be done to optimize the profile level and stirrup locations; and usage with high concrete grade for effective exploitation.

### ARTICLE INFO

Article history: Received 2 May 2020 Revised 25 May 2020 Accepted 31 May 2020

Keywords:
Reinforced cement concrete
ANSYS
MS rebar
HYSD rebar
PSWC rebar
Rib configuration

### 1. Introduction

Reinforced concrete is a composite material in which concrete's relatively low tensile strength and ductility are counteracted by the inclusion of reinforcement having higher tensile strength and ductility as mentioned by Meddah and Bencheikh (2009). The reinforcement used, is steel reinforcing rebar and is usually embedded passively in the concrete before it sets. For many years, it has been utilized as an economical construction material in

<sup>\*</sup> Corresponding author. E-mail address: r.sarvat@gmail.com (S. Gull) ISSN: 2548-0928 / DOI: https://doi.org/10.20528/cjcrl.2020.03.002

one form or another in buildings, bridges, and many other types of structures throughout the world as explained by Nanni (2003). In addition to being readily obtainable, reinforced concrete has been universally accepted because it can be moulded essentially into any shape or form, is inherently rigid, and is inherently fireresistant as defined by Gagg (2014). In reinforced concrete, the tensile strength of steel and the compressive strength of concrete work together to allow the member to sustain the stresses over considerable spans. However, failures in concrete structures do still occur as a result of premature reinforcement corrosion as explained by Song and Saraswathy (2007).

"Durability of reinforced concrete structures is a pervasive and universal problem. Many concrete structures deteriorate prematurely, and repair and maintenance costs amount to substantial proportions of public and private sector budgets. Many researchers suggests, reasons for durability problems as poor understanding of deterioration processes, inadequate acceptance criteria of site concrete, and changes in cement properties and construction practices" as mentioned by Hobbs (2001). Durability problems cover a wide range including attack by external destructive agents (e.g. sulphates), internal material incompatibilities (e.g. alkali-aggregate reaction), and aggressive environments such as freeze-thaw etc.; Nevertheless, the greatest threat to durability of concrete structures is undoubtedly corrosion of embedded reinforcing steel, leading to cracking, staining, and spalling of the cover concrete (Neville, 1987). This in turn can lead to unserviceable structures that may be compromised in respect of safety, stability, and aesthetics.

In reinforced concrete structures, reinforcing steel provides the tensile properties that are needed in structural concrete. It prevents the failure of concrete structures which are subjected to tensile and flexural stresses due to traffic, winds, dead loads, and thermal cycling. Materials used for reinforcement are usually roughly textured to encourage the concrete to fully adhere as mentioned by Garden et al. (1998). However, when reinforcement corrodes, the formation of rust leads to a loss of bond between the steel and the concrete and subsequently delamination and spalling as explained by Goyal et al. (2018). If this is left unchecked, the integrity of the structure can be affected. It is also associated with reduction in the cross sectional area of steel which in reduces strength capacity of RC structures. Hence it is necessary to identify the causes for corrosion as early as possible and implement corrosion protection techniques to safeguard the structures. The major factors influencing corrosion process of steel reinforcement in reinforced concrete structures are pore solution of concrete, moisture, chloride content, carbon dioxide, components of concrete, concrete resistivity, thickness and defects of cover concrete and temperature as mentioned by Marcos-Mason et al. (2018). Apart from the above mentioned factors, corrosion process can also be influenced by the surface deformations on the steel reinforcement used in the reinforced concrete as explained by Zhao et al. (2011). It can be recognized that the problem of early distress due to corrosion in reinforced concrete structures came into existence after the introduction of high strength rebars

with surface deformations. These rebars can be easily identified by the presence of lugs or protrusions on their surface. Compared with plain rebars, rebars with surface deformations corroded faster. These deformed rebars with a stepped profile have space concentrators on the surfaces of projections which represents the sites of preferential formation of cracks. Presence of these projections on the surface of the rebars, are the areas with high stress concentration and consequently it creates non-uniform stress distribution, paving way for formation of anode and cathode which becomes the birth place for corrosion. These rebars with surface lugs are preferred, even though they are susceptible to corrosion because of their strength and need for limiting the anchorage or bond length or lap length. A problematic feature of these rebars is that the thin edges of the lugs, which are often damaged during the making, transportation and handling. The damaged regions lead to the creation of sites with potential differences and corrosion process commences, gradually the whole lengths of bars are covered with rust. Fig. 1(a) shows the view of new and Fig. 1(b) shows the view of corroded twisted rebar.





**Fig. 1.** (a) View of new rebars; (b) Corroded twisted rebar.

Although, the yield strength as well as the bond strength of HYSD rebars are higher as compared to those of the plain round mild steel straight rebars, there are certain durability issues related to the use of HYSD rebars in reinforced concrete structures; problems of early distress and associated failures of reinforced concrete structures, built using HYSD bars due to early corrosion of the HYSD bars, have been reported by Kar (2012). With the objective of achieving an alternative solution for overcoming the early corrosion problem in using HYSD rebars in reinforced concrete structures, a new type of reinforcing steel bar (named as PSWC rebar) with normal plain round surface having slightly curved axis has been proposed by Kar (2019). Fig. 2 shows the view of a PSWC rebar.



Fig. 2. View of a PSWC bar.

PSWC rebars are proposed with an objective of overcoming the above mentioned defects. PSWC rebar is a rebar for durable concrete construction at zero cost addition and much more. PSWC bar is characterized by its plain surface and a deformed axis to give it a gentle wave-type configuration. The offset (excursion from the original straight axis) is merely a few 4-8 millimeters. The plain surface of the PSWC rebar overcomes the problems due to corrosion because of uniform stress distribution throughout the length of the rebar. PSWC rebars can solve both, strength and durability problems. The use of PSWC rebars could possibly make the reinforced concrete structure more ductile than concrete structures which may be reinforced with conventional (with straight axis) rebars.

In this experimental study, PSWC bar with 4mm deformation and 6mm deformation are used. Fig. 3(a) shows view of PSWC rebar with 4mm and Fig. 3(b) shows view of PSWC rebar with 6mm deformation.





**Fig. 3.** (a) View of PSWC rebar with 4mm deformation; (b) View of PSWC rebar with 6mm deformation.

The scope of present investigation is to assess the flexural behaviour of RCC elements reinforced with PSWC rebars. The flexural performance of RC beams of size 1000mm x 150mm x 150mm reinforced with PSWC rebars with 4mm and 6mm deformation level is studied by conducting test as per IS:516-1959 (method of test for strength of concrete) under four point loading method. The performance of PSWC rebar reinforced elements are compared with beams reinforced with mild

steel rebars, HYSD rebars with spiral and diamond rib configuration to assess the viability of PSWC rebars to replace conventional reinforcement and subsequent use for structural application. The test results are validated by numerical analysis with the help of ANSYS software. In each category three beams are cast and totally 15 beams are subjected to flexure test. The performance evaluators in this study are first crack load, deflection at first crack load, ultimate load carrying capacity, deflection at ultimate load, load-deflection behaviour, load-strain behaviour and failure pattern. The followings are the category of RC elements subjected to flexure test:

- RC beams reinforced with mild steel bars,
- RC beams reinforced with PSWC rebar of 4mm deformation,
- RC beams reinforced with PSWC rebar of 6mm deformation,
- RC beams reinforced with spiral rib HYSD rebars.
- RC beams reinforced with diamond rib HYSD rebars.

### 2. Material Properties and Mix Design

PSWC bars with 4mm and 6mm deformation level were supplied by M/S. Engineering Consultants, Calcutta. All other materials were procured locally and used. Ordinary Portland cement (OPC) - 53 grade, river sand, single graded coarse aggregate, potable water, mild steel rebars of 12 mm diameter, parallel/spiral rib HYSD rebars of 12 mm diameter, diamond rib HYSD rebars of 8 mm, 10 mm, 12 mm diameter, PSWC rebar of 10 mm and 12 mm diameter with 4 mm deformation, PSWC rebar of 10 mm and 12 mm diameter with 6 mm deformation. The basic properties of the cement such as consistency, initial setting, final setting and specific gravity were found as per IS:4031-1989 (methods of physical test for hydraulic cement), IS:269-1989 (specific gravity of cement ) and IS:516-1959 (compressive strength of cement). The properties of fine aggregate and coarse aggregate are found as per IS:2386 (methods of test for aggregate for concrete). The grading is conforming to IS:2720 (part IV) – 1985. Table 1 shows the property of cement, fine aggregates and coarse aggregates.

Based on the material property test results, mix design for M25 concrete was formulated for 1m<sup>3</sup> of concrete as per IS:10262-2009 as shown in Table 2.

Slump test was conducted to measure the consistency of concrete. Trial mix was made for determining the slump for the formulated design mix ratio. The trial mix for M25 grade of concrete was made with 63.5% of coarse aggregate and 36.5% of fine aggregate which offers a slump of 80 mm, which is found to be optimum for hand mixing.

Each rebar of 12 mm and 10 mm size of mild steel of grade  $f_y$  = 250 MPa, HYSD parallel ribs, HYSD diamond ribs of grade  $f_y$  = 500 MPa were tested to determine the corresponding chemical composition and also tension test was conducted using UTM to check the physical property of specimens. The chemical composition and tension test results were found in optimum range as shown in Tables 3 and 4 respectively.

	_		
S. No.	Constituent	Properties/Obtained Value	BIS Recommended Range
1	Cement	Specific gravity –3.15 Consistency –32%	> 3.15
2	Coarse Aggregate	Specific gravity–2.797 Waterabsorption–0.25% Grading conforming to IS:2386-1963	2.4-2.6
3	Fine Aggregate	Fineness modulus-3.15 Specific gravity–2.547 Waterabsorption-6% Conforming to Zone -I Grading conforming to IS:383-1970	2.9-3.2 2.4-2.6 -

**Table 1.** Material properties of cement, fine aggregate and coarse aggregate.

**Table 2.** Design mix proportions for 1m<sup>3</sup> of concrete.

Water	Cement	Fine Aggregate	Coarse Aggregate
153	340	695	1280
0.45	1	2.04	3.76

**Table 3.** Chemical composition test results.

Characteristic Test	MS rebar results	HYSD rebar results (Parallel ribs)	HYSD rebar results (diamond ribs)
Carbon (%)	0.284	0.203	0.222
Manganese (%)	0.553	0.696	0.567
Silicon (%)	0.157	0.208	0.104
Sulphur (%)	0.028	0.024	0.024
Phosphorous (%)	0.036	0.033	0.032
Chromium (%)	0.190	0.092	0.186
Nickel (%)	0.099	0.068	0.069
Molybdenum (%)	0.017	0.013	0.016

Table 4. Tension test results.

Type of bar		Properties		
Type of bar	Yield strength (MPa)	Ultimate strength (MPa)	% Elongation	% Reduction
Mild Steel	466.72	583.40	27.5	54.23
HYSD Parallel Ribs	498.36	622.96	22.5	55.45
HYSD Diamond Ribs	547.77	684.72	26.2	54.90

### 3. Experimental Program

Concrete is relatively strong in compression and weak in tension. In reinforced concrete members, only partial amount of tensile stresses are resisted by concrete, rest of the whole tensile stresses are resisted by steel reinforcing bars. However, tensile stresses are developed in the concrete due to drying shrinkage, rusting of steel reinforcement, temperature gradients, etc. Therefore, the knowledge of tensile strength of concrete is essential.

The tensile strength of concrete cannot be measured directly; hence beams are tested for flexural strength property of concrete. Flexural strength test is carried out according to IS:516-1959. The code specifies two-point loading for measuring flexural strength of concrete.

Different types of rebars were used as reinforcement and comparisons were made with PSWC rebars of 4mm and 6mm deformation. The different types of rebars used in the beam specimens are listed below in the Table 5.

**Table 5.** Different types of rebars used as reinforcement.

S. No.	Type of reinforcement
1	Mild steel rebars
2	High yield strength rebars with spiral rib configuration
3	High yield strength rebars with diamond rib configuration
4	PSWC rebar with 4mm deformation
5	PSWC rebar with 6mm deformation

### 3.1. Specimen details

The specimens were cast to a size of 150mm wide, 150mm deep and length of 1000mm. The clear cover of the beam was provided as 30mm. The bottom reinforcement was two nos. of 12mm diameter and the top reinforcement was two nos. of 10mm diameter. Two legged vertical stirrups were provided at a spacing of 150mm center to center for conventional rebars and 105mm center to center for PSWC rebars. Reinforcement details of the specimen are shown in Fig. 4 and details for different types of beams are listed in the Table 6.

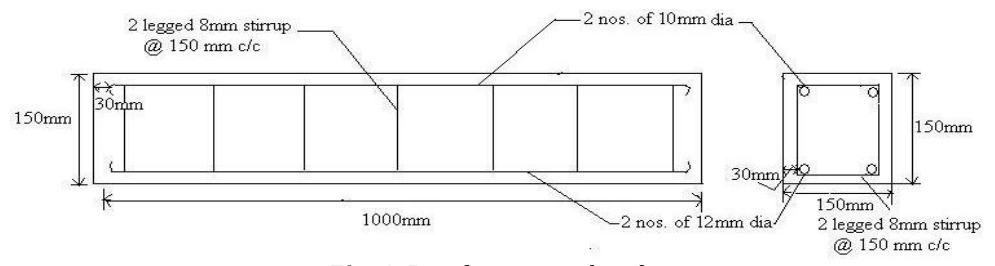


Fig. 4. Reinforcement details.

**Table 6.** Reinforcement details for different types of beams.

S. No.	Type of reinforcement	$A_{SC}$	$A_{St}$	$A_{SV}$	No. of specimen
1	Mild steel rebars	2 nos. of $10$ mm $\Phi$	2 nos. of $12\text{mm}\Phi$	2 legged 8mm stirrups @150mm c/c	3
2	Spiral rib HYSD rebars	2 nos. of $10\text{mm}\Phi$	2 nos. of $12\text{mm}\Phi$	2 legged 8mm stirrups @150mm c/c	3
3	Diamond rib HYSD rebars	2 nos. of $10\text{mm}\Phi$	2 nos. of $12\text{mm}\Phi$	2 legged 8mm stirrups @150mm c/c	3
4	PWSC-bar (4mm def.)	2 nos. of $10\text{mm}\Phi$	2 nos. of $12\text{mm}\Phi$	2 legged 8mm stirrups @105mm c/c	3
5	PWSC-bar (6mm def.)	2 nos. of $10\text{mm}\Phi$	2 nos. of $12\text{mm}\Phi$	2 legged 8mm stirrups @105mm c/c	3

Notations:  $A_{sc}$ -reinforcement in compression zone;  $A_{st}$ -reinforcement in tension zone;  $A_{sv}$ -area of stirrups;  $\Phi$ -diameter of rebar.

### 4. Materials and Preparation

Moulds were fabricated in the strength of materials laboratory. One inch thick plywood with polymer painted for protection was used. Fig. 5 shows the picture of the fabricated moulds.

Electrical resistance type strain gauge with 5mm length and 120 ohms resistance was used. The strain gauge was located at the center of one of the longitudinal reinforcements to measure longitudinal strain. A specific procedure was followed for fixing of strain gauges and it was applied for all types of specimen before casting. Fig. 6 shows the procedure for fixing of strain gauge.

Different types of rebars were procured from various places to the laboratory and reinforcement cage was fabricated in the nearby site. The tension reinforcement, compression reinforcement and stirrups were bent according to the requirement after which the cage was fabricated. Fig. 7(a-e) shows the picture of reinforcement cage of different types of bars.

A total of 15 beams were casted i.e. three in each category. The strain gauge of 5mm gauge length and 120 ohm resistance was fixed at the centre of one of the tension reinforcements. All the beams were casted in laboratory, prior to casting the inner walls of the moulds were coated with lubricating oil to prevent adhesion with hardening concrete. The materials were given a proper hand mixing and the concrete was placed in three equal layers and was given intact compaction with tamping rod until good compaction was obtained. All the beams were de-moulded after 24 hours. The beams were water cured with jute bags for a period of 28 days after casting.

The tests were carried out in Universal testing machine with 100 tonnes capacity. The bed of the testing machine was provided with two steel rollers, 38 mm in diameter, on which the specimen was supported, and these rollers were mounted at a distance of 600mm centre to centre. The load was applied through two similar rollers mounted at the third points of the supporting span spaced at 200mm centre to centre. The load was divided

equally between the two loading rollers which were connected by 30 mm thick plate on top. A load cell with 50 tonnes capacity was mounted on the plate fixed at the top of the rollers. A sensitive dial gauge with 0.01 mm least count was placed at the center of the beam to measure mid-span deflection. A strain gauge length of 5 mm with

120 ohm resistance was fixed at the center of bottom reinforcement, which was connected to the Universal Data Acquisition and Control System which in turn connected to the computer. The load-strain behaviour was obtained automatically from the system attached with 16 channel data logger. The test setup for flexure test is shown in Fig. 8.



Fig. 5. View of fabricated moulds.

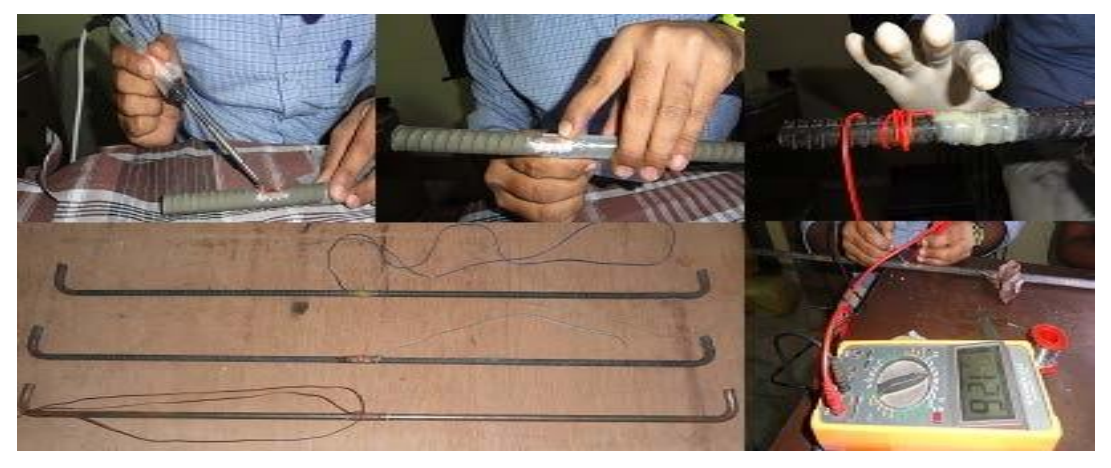


Fig. 6. Fixing of strain gauge.



(a) View of PSWC 4mm deformation reinforcement cage



(b) View of PSWC 6mm deformation reinforcement cage



(c) View of HYSD diamond rib reinforcement cage



(d) View of Mild steel reinforcement cage



(e) View of HYSD parallel rib reinforcement cage

**Fig. 7.** Reinforcement cage for different types of rebar.

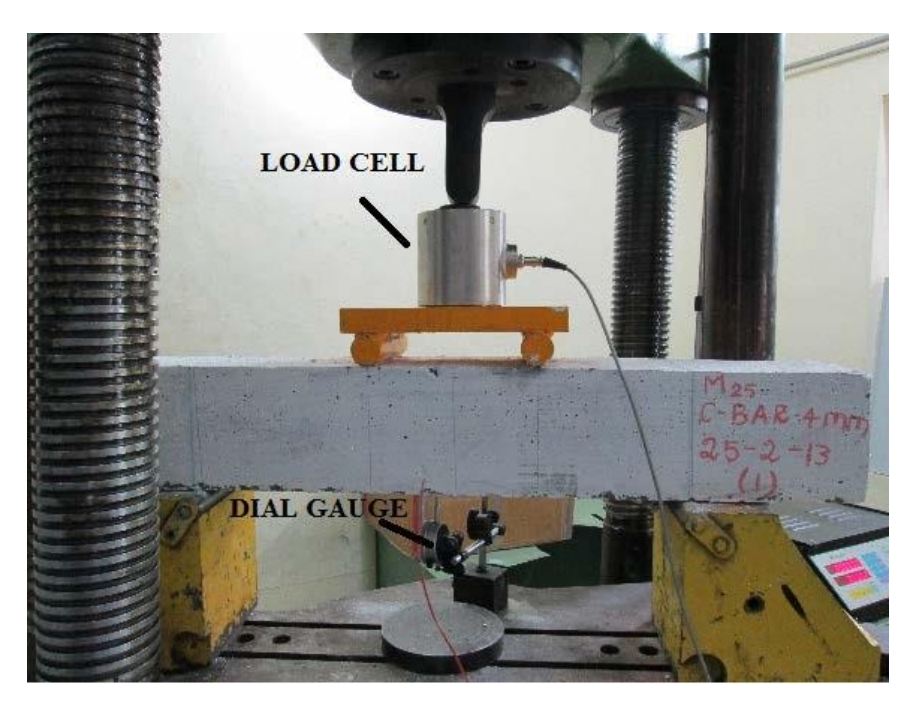


Fig. 8. Flexural strength test setup.

### 5. Test Procedure

The dimensions of each specimen were noted before testing. The specimens were given marking at the center, supports and along the roller axis. The bearing surfaces of the supporting and loading rollers was wiped clean, and any loose sand or other material was removed from the surfaces of the specimen where they are to make contact with the rollers. The specimen was then placed in the machine in such a manner that the load shall be applied to the uppermost surface as cast in the mould, along two lines of rollers spaced 200mm apart. The axis of the specimen was carefully aligned with the axis of the loading device. The load was applied gradually without shock and was increased until the specimen fails. The maximum load applied to the specimen during the test was recorded as ultimate load. The appearance of the fractured faces of concrete and any unusual features in the type of failure was noted.

The flexural strength of the specimen shall be expressed as the modulus of rupture  $f_b$ , which, if 'a' equals the distance between the line of fracture and the nearer support, measured on the centre line of the tensile side of the specimen, in cm, shall be calculated to the nearest 0.5 kg/sq cm as follows:

$$f_b = p l / b d^2 \tag{1}$$

when 'a' is greater than 20.0 cm for 15.0 cm specimen, or greater than 13.3 cm for a 10.0 cm specimen, or when 'a' is less than 20.0 cm but greater than 17.0 cm for 15.0 cm specimen, or less than 13.3 cm but greater than 11.0 cm for a 10.0 cm specimen.

$$f_b = 3p \ a \ / \ b \ d^2 \tag{2}$$

where d is measured depth in cm of the specimen at the point of failure, l is length in cm of the span on which the specimen was supported, and p is maximum load in kg applied to the specimen.

If 'a' is less than 17.0 cm for a 15.0 cm specimen, or less than 11.0 cm for a 10.0 cm specimen, the results of the test shall be discarded.

### 6. Analytical Investigation

Experimental based analysis has been widely used as a means to find out the response of individual elements of structure. This method is time consuming and the use of materials can be quite costly. In recent years, the use of finite element analysis has increased due to progressing knowledge and capabilities of computer software and hardware and has become the choice of modern engineering tools for the researcher to analyze concrete structural components.

The use of computer software to model these elements is much faster, and extremely cost-effective.

### 6.1. Modelling and analysis of RC beam reinforced with conventional rebars and PSWC rebars using ANSYS

Modelling of the reinforced concrete beam was done using ANSYS software. The reinforcement was modelled exactly as embedded in the concrete with sufficient cover thickness on either side. The beam was subjected to two point loading according to the Indian standards codal provisions. The analysis is made for both conventional rebars and PSWC rebars, and the results of the analysis are validated and compared with the results of the experimental investigation.

Solid65 element was used to model the concrete material, since it has capability of both cracking in tension and crushing in compression. Solid65 element has 8 nodes with three degrees of freedom at each node – translations in the nodal x, y, and z directions. Fig. 9 shows the picture of element Solid65.

The Link8 spar element was used to represent the reinforcing steel rebar. Two nodes are required for this element such that each node has three degrees of freedom, translations in the nodal x, y, and z directions. The element is also capable of plastic deformation. Fig. 10 shows the picture of element link spar 8. The beam specimens modeled in ANSYS software are shown in the Figs. 11-15.

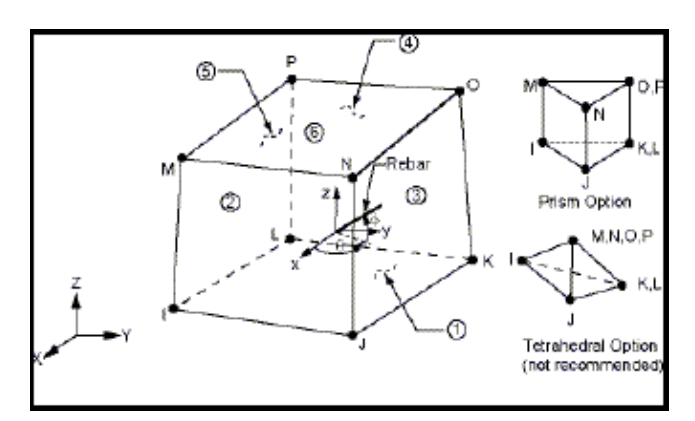


**Fig. 9.** Element type: Solid65.

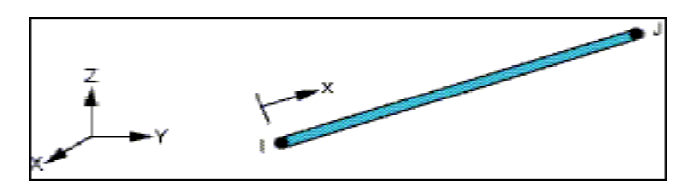


Fig. 10. Element type: Link8.

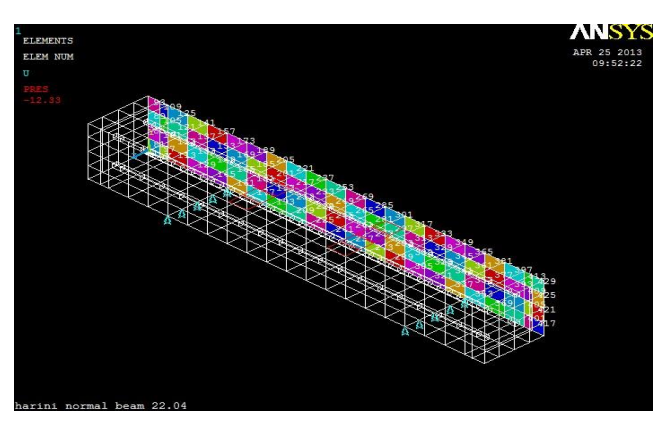


Fig. 11. Reinforcement model of conventional bar.

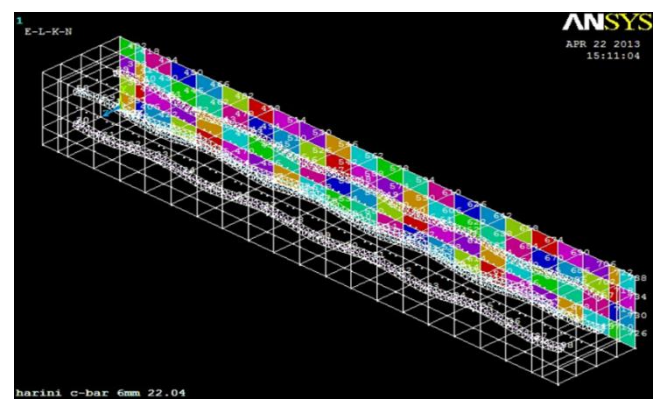


Fig. 12. Reinforcement model of PSWC bar.

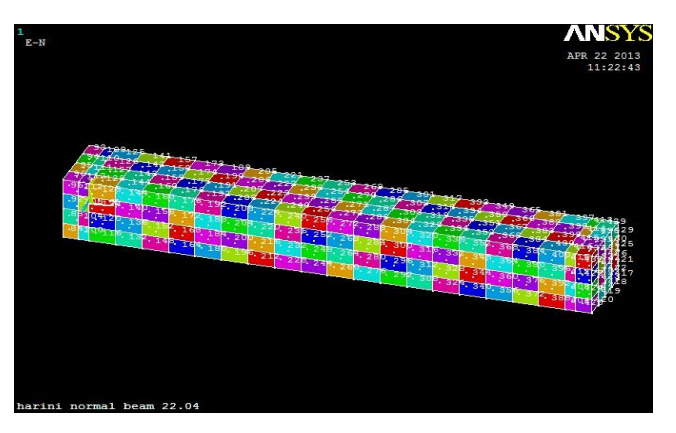


Fig. 13. Concrete block.

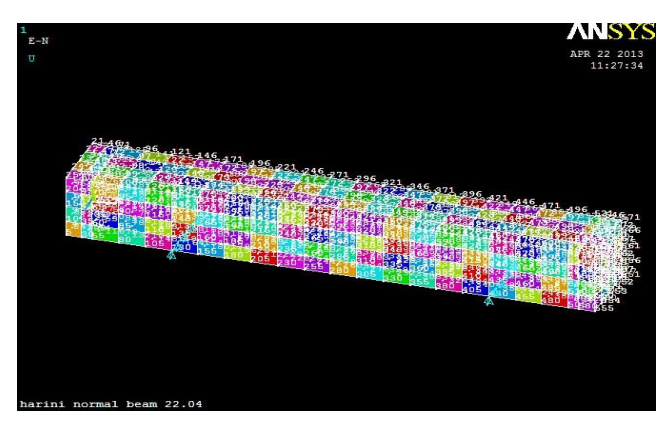


Fig. 14. Support condition.

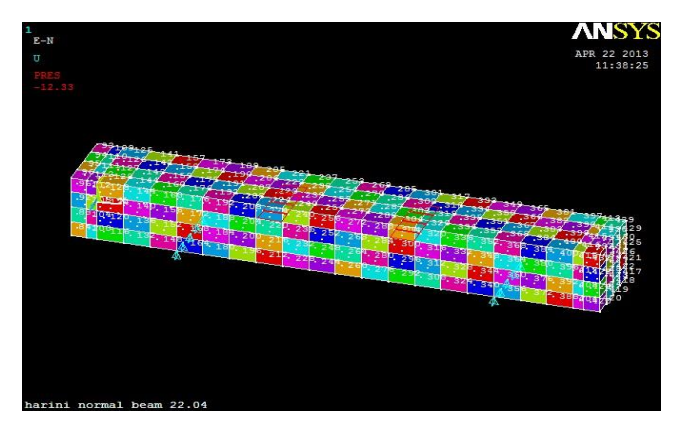


Fig. 15. Loading diagram.

### 7. Results and Discussion

The flexural performance of PSWC rebars was evaluated and compared with different types of rebars. A total of 15 beams of size 1000mm x 150mm x 150mm were casted and subjected to flexural test according to IS:516-1959 under four point loading. The categories of beams tested include:

- RC beam with PSWC rebar (4 mm deformation),
- RC beam with PSWC rebar (6 mm deformation),
- RC beam with mild steel rebars,
- RC beam with spiral/parallel rib HYSD rebars,
- RC beam with diamond rib HYSD rebars.

The experimental results are compared with analytical results obtained from ANSYS.

### 7.1. Flexural strength test

The beam specimens were subjected to four-point loading as per IS:516-1959 to assess the flexural behaviour. The evaluation parameters include load-deflection behaviour, first crack load, ultimate load, load-strain behaviour & crack pattern. Table 7 exhibits the observation on flexure test with respect to load carrying capacity. It can be observed from the table, the first crack load of PSWC rebar reinforced beams are found to be in the range of 45kN-55kN which is appreciably high than that of HYSD rebar beams and mild steel rebar beams, while the ultimate load capacity of PSWC rebar reinforced concrete beams are found to be appreciably less than that of

HYSD rebar beams and mild steel rebar beams. This could be attributed due to low compressive strength of concrete and yielding nature of PSWC rebars.

The observation on ultimate load and mid-span deflection are explicit in the Table 8. It can be observed that deflection at first crack load is marginally high for beams with PSWC rebars as compared to beams with mild steel and HYSD rebars. Significant increase in deflection level for beams with PSWC rebars at ultimate load irrespective of deformation level as compared to beams with mild steel and HYSD rebars exhibiting improved ductility.

Figs. 16-20 show the load-deflection behaviour at mid-span for beams with HYSD rebars, mild steel rebars, and PSWC rebars with 4mm and 6mm deformation.

<b>Table 7.</b> Observation on flexure test with respect to load carrying capacity.
---

S. No.	Type of specimen	First crack load (kN)	Ultimate load (kN)
1	Beams with spiral rib HYSD rebars	51	165
2	Beams with diamond rib HYSD rebars	40	185
3	Beams with mild steel rebars	55	165
4	Beams with PSWC rebars (4mm deformation)	56	130
5	Beams with PSWC rebars (6mm deformation)	45	120

**Table 8.** Observation on ultimate load and mid-span deflection.

S. No.	Type of specimen	First crack load (kN)	Deflection at first crack (mm)	Ultimate load (kN)	Mid-span deflection (mm)
1	Beams with spiral rib HYSD rebars	51	0.35	165	4.98
2	Beams with diamond rib HYSD rebars	40	0.25	185	4.28
3	Beams with mild steel rebars	55	0.27	165	3.08
4	Beams with PSWC bars (4 mm deformation)	56	0.54	130	7.10
5	Beams with PSWC bars (6 mm deformation)	45	0.48	120	7.20

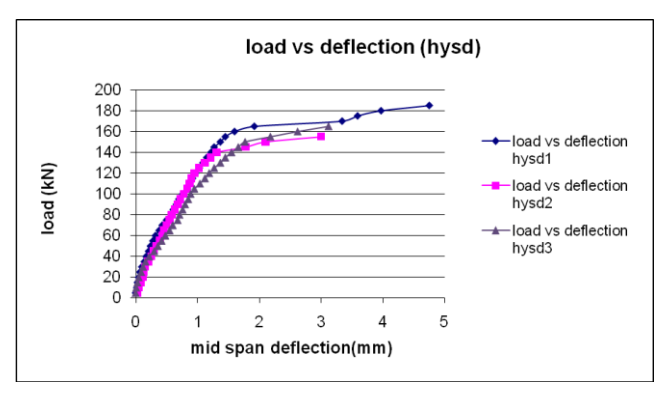


**Fig. 16.** Load-deflection behaviour for beams with rib HYSD rebars.

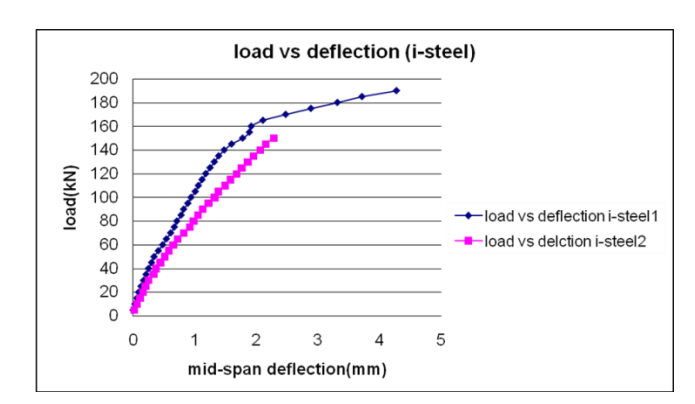


**Fig. 17.** Load-deflection behaviour for beams spiral with diamond rib HYSD rebars.

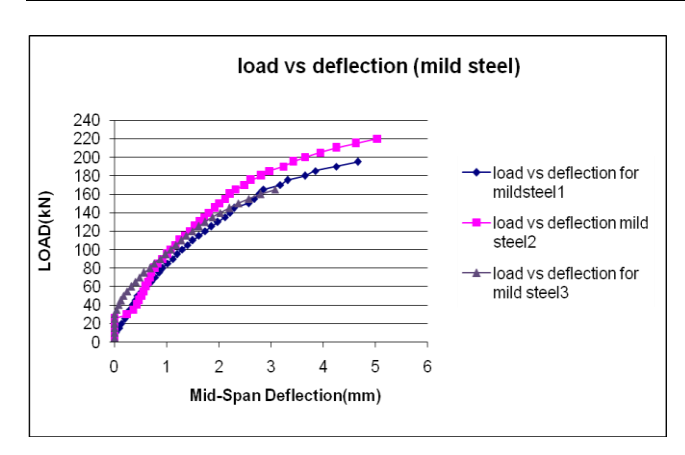


**Fig. 18.** Load-deflection behaviour for beams with mild steel rebars.

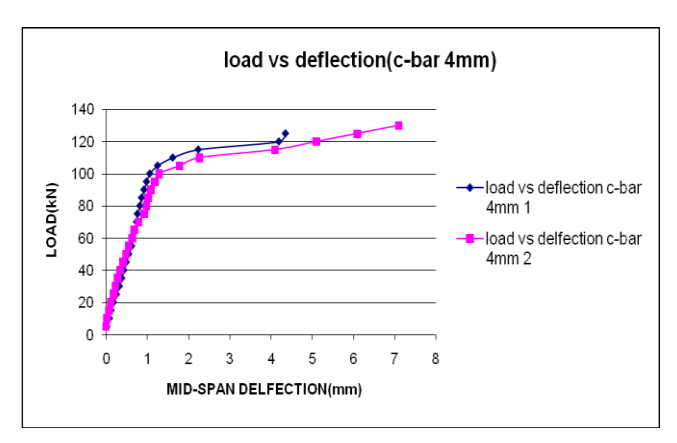


**Fig. 19.** Load-deflection behaviour for beams with PSWC rebar (4mm deformation).

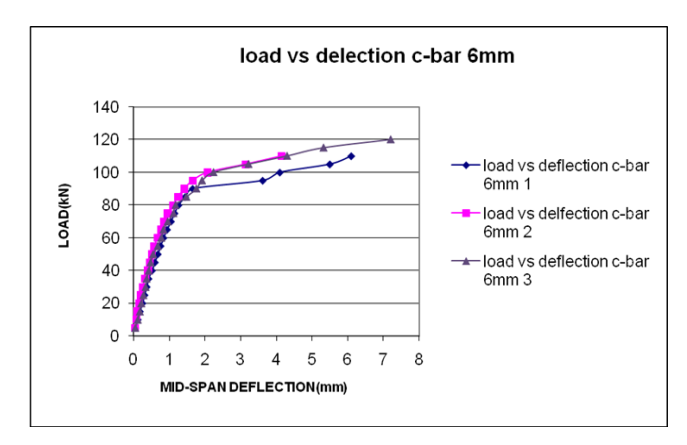


**Fig. 20.** Load-deflection behaviour for beams with PSWC rebars (6mm deformation).

From Figs. 16-20, it can be observed that in all the specimens, the first crack load was found to be in the range of 40 kN to 55 kN. The first crack load of PSWC rebar reinforced beams are found to be appreciably higher than that of HYSD rebar beams and the deflection recorded corresponding to those loads are higher, indicating the ductile behaviour of PSWC rebars .On further increase of load beyond first crack load, the deflection has increased rapidly upon small increase of load.

From Figs. 16 and 17, the linear behaviour exists up to a load of 140 kN for beams with spiral and diamond rib HYSD rebars. On further increase of load, appreciable deflection was recorded for small increment of load until failure. It can be seen from the Fig. 18, deflection was found to be negligible up to a load of 25 kN, and from there on it has increased gradually until the failure and almost a linear behaviour has been observed up to 180kN, which indicates, for appreciable increase of load, there is rapid increase in the deflection which registers brittle failure of beams.

Figs. 19 and 20 exhibit the Load - deflection behaviour of beams with PSWC rebar (4mm and 6mm deformation). Almost a linear behaviour exists up to a load of 100kN, upon further increase of load, softening of curve has emerged which indicates for small increase of load there is rapid increase in deflection. The deflection pattern registered before failure reveals improved ductile behaviour for beams with PSWC rebars irrespective of deformation level.

### 7.2. Comparison of load-deflection behaviour of beams with PSWC rebars, HYSD rebars and mild steel rebars

The load vs. deflection behaviour of PSWC rebar beams is compared with conventional HYSD rebar beams and mild steel rebar beams. The various combinations of load-deflection behaviours are plotted in Figs. 21-28.

Figs. 21-28 show the combined load vs. deflection behaviour of HYSD, mild steel and PSWC rebar reinforced beams. From Figs. 24-25, it can be seen that, the load deflection behaviour of PSWC rebar beams is found to be similar to that of other conventional rebar beams especially with spiral rib and diamond rib HYSD rebar beams. It can be observed that, large deflections are recorded for small ultimate loads for PSWC rebar reinforced beams; this could be due to the ductile behaviour of beams, which is imparted by the deformed profile of PSWC rebars. A well–defined and almost a similar load-deflection behaviour has been recorded for PSWC rebar reinforced beams, although there is marginal reduction in ultimate load when compared with HYSD and mild steel rebar reinforced beams.

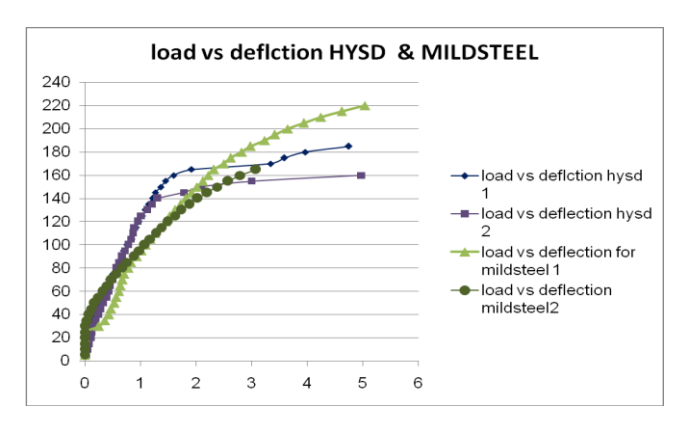


**Fig. 21.** Load-deflection behaviour of beams with spiral rib HYSD rebars and mild steel rebars.

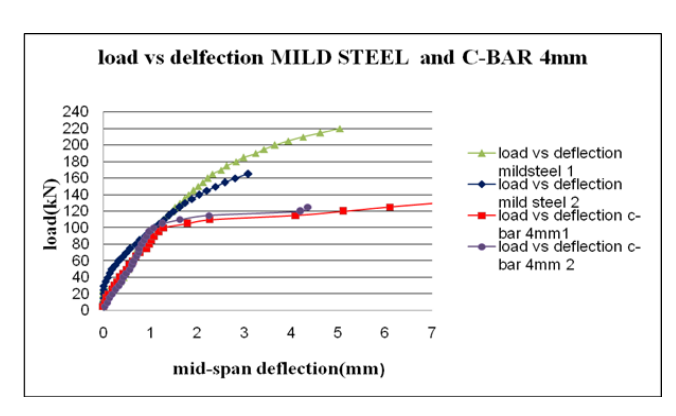


**Fig. 22.** Load-deflection behaviour of beams with mild steel rebars and PSWC rebars (4mm deformation).



**Fig. 23.** Load-deflection behaviour of beams with mild steel rebars and PSWC rebars (6mm deformation).

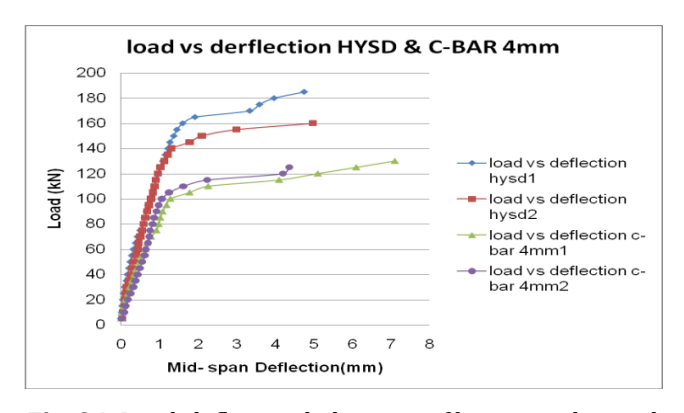


**Fig. 24.** Load-deflection behaviour of beams with spiral rib HYSD rebars and PSWC rebars (4mm deformation).

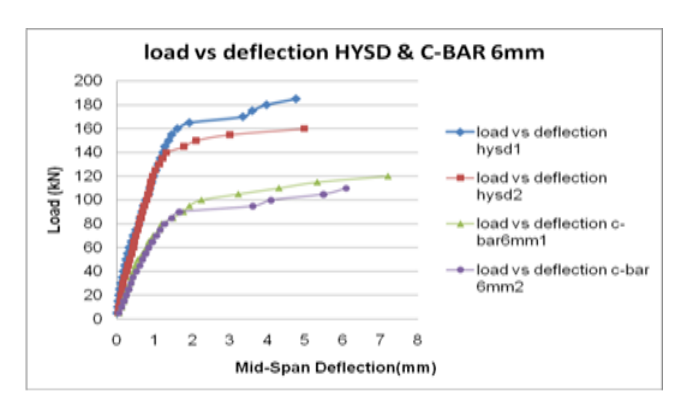


**Fig. 25.** Load-deflection behaviour of beams with spiral rib HYSD rebars and PSWC rebars (6mm deformation).

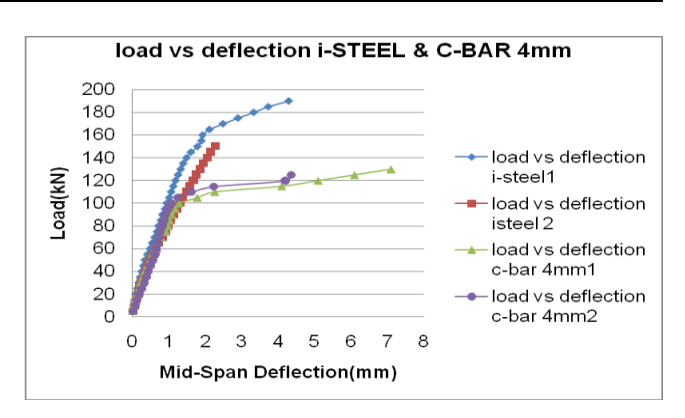


**Fig. 26.** Load-deflection behaviour of beams with diamond rib HYSD rebars and PSWC rebars (4mm deformation).

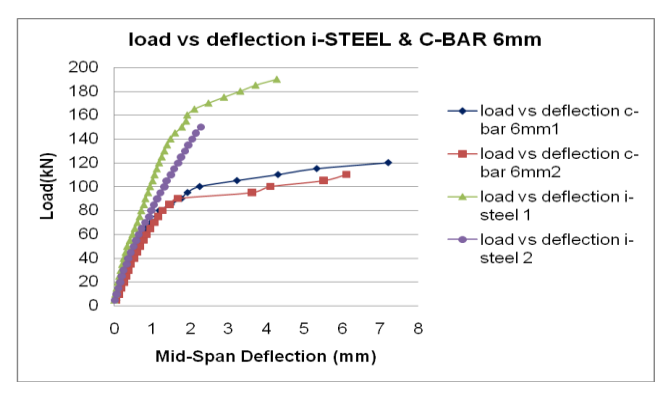


**Fig. 27.** Load-deflection behaviour of beams with diamond rib HYSD rebars and PSWC rebars (6mm deformation).

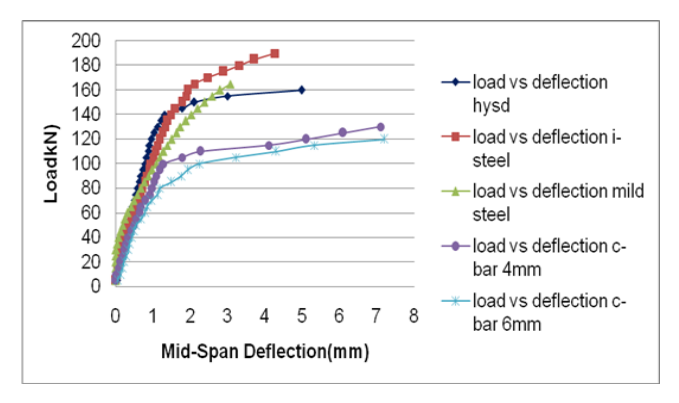
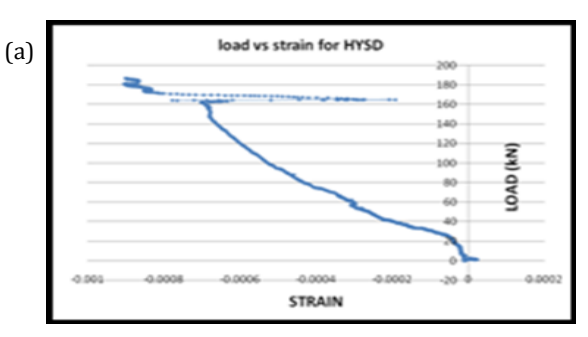


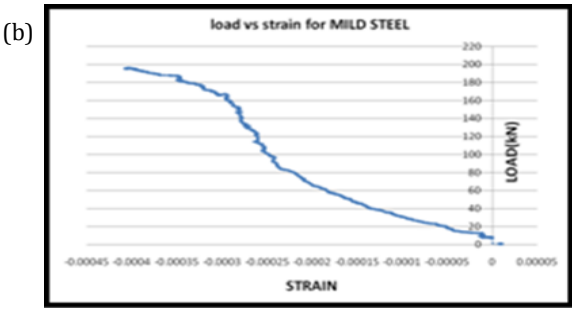
**Fig. 28.** Load-deflection behaviour of beams with mild steel rebars, HYSD rebars and PSWC rebars.

### 7.3. Load-strain behaviour

The strain gauge was fixed at the centre of the reinforcement to record load vs. strain behaviour. This was recorded automatically by the system connected to data logger, through digital data acquisition system. Fig. 29(a-c) shows the load vs. strain behaviour of beams with HYSD, mild steel and PSWC rebar, respectively. From Fig. 29(a-b), it can be inferred that in case of HYSD rebar beams, there is a gradual increase in the strain upon increase of load and yielding of reinforcements was not observed during the test. For PSWC rebar reinforced beams, the Load vs. strain behaviour of PSWC rebar with 4mm deformation is shown in the Fig. 29(c). It

is observed that strain has increased rapidly in the initial stages of load application and the yield plateau recorded shows the improved ductile behaviour of PSWC rebars. Further studies have to be carried for better understanding of load-strain behaviour of PSWC rebars.





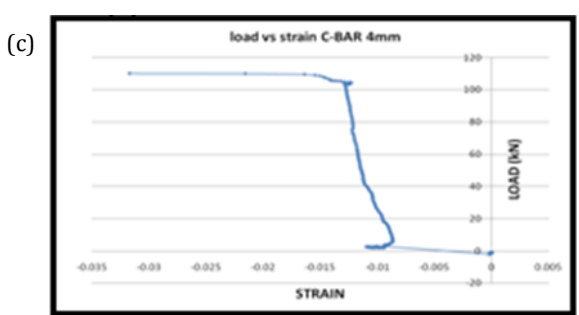
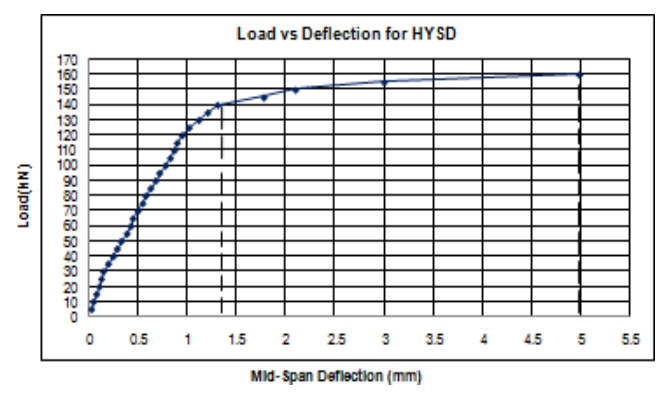


**Fig. 29.** Load vs. strain behaviour: (a) HYSD; (b) Mild steel; (c) PSWC rebar (4mm deformation) reinforced beams.

In this study, the displacement ductility was investigated. Table 9 shows the ductility and energy absorbing capacity of the HYSD rebar beams, mild steel rebar beams and C-bar beams and Fig. 30(a-d) shows the load-deflection curve with projected yield deflection and ultimate deflection for the tested beams and ductility calculations. It can be observed from the Fig. 30(a-d) that, the ductility has immensely increased for beams reinforced with C-bars than beams reinforced with HYSD rebars and mild steel rebars. It is registered from the curves of above figures that C-bar reinforced beams had a significant increase in energy absorbing capacity. This could be due to the large deflection recorded for small increment of load in the post peak region.

### 7.4. Failure mode and crack pattern

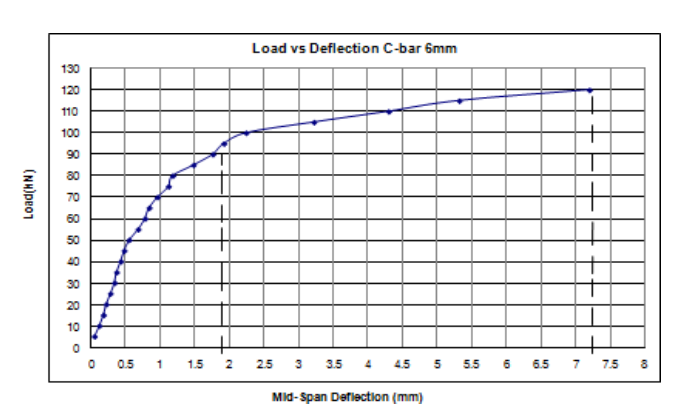
Failure modes of beams with spiral rib and diamond rib conventional HYSD rebars, mild steel rebars and PSWC rebars are tabulated in the Table 9.



(a) Load vs. deflection behaviour for Spiral Rib HYSD rebar beams



(b) Load vs. deflection behaviour for diamond rib HYSD rebar beams



(c) Load vs. deflection behaviour for PSWC rebar (4mm deformation) beams



(d) Load vs. deflection behaviour for PSWC rebar (6mm deformation) beams

**Fig. 30.** Load-deflection behaviour of tested beam for ductility calculations.

S. No.	Type of specimen	Displacement Ductility	Energy Absorption Capacity (kN-mm)
1	Beams with spiral rib HYSD rebars	3.80	12.45
2	Beams with diamond rib HYSD rebars	2.26	20
3	Beams with mild steel rebars	-	-
4	Beams with PSWC rebars (4mm deformation)	5.54	33
5	Beams with PSWC rebars (6mm deformation)	3.75	31.3

**Table 9.** Ductility and energy absorption capacity of tested beams.

Figs. 31-35 show the failure mode and crack pattern for different categories of beams. It is observed that HYSD rebar beams had undergone diagonal shear failure while the mild steel and PSWC rebars reinforced beams had undergone flexural failure. In case of HYSD rebar beams, cracks originated near the support and propagated in the same region with further application of load, while in case of mild steel and PSWC rebar reinforced beams cracks originated at the centre of the beam registering tension failure and new carks propagated near to the support on further application of load. It can be visualized from the figures that the failure mode of both, the conventional rebar such as HYSD rebar (diamond rib) and mild steel rebar reinforced concrete beams and that of PSWC rebar reinforced concrete beam was found to be nearly similar.

It is to be noted that crack width of the PSWC rebar reinforced beams were found be less than that of conventional rebar reinforced beams. An unusual behaviour was captured in mild steel reinforced beams, the failure was under flexure but at one end of the beam, concrete was pushed out, which could be due to the 'L'bent provided at the end of the rebars. This behaviour was not captured in case of PSWC-rebars reinforced beams although the failure was under flexure. In PSWC rebar beams, the crack has originated at the trough portions of the curve, which tends to get straight while the beam is deflected. These portions exert pressure on the cover concrete while straightening and only crack formation commences in those regions while preventing pushing out of concrete.

### 7.5. Analytical results

It is observed that analytical results also give good agreement with experimental results. Fig. 36(a-c) shows the deflection of different beams obtained from the analysis.



Fig. 31. Failure pattern of beams reinforced with spiral rib HYSD rebars.



Fig. 32. (continued).



Fig. 32. Failure pattern of beams reinforced with mild steel rebars.

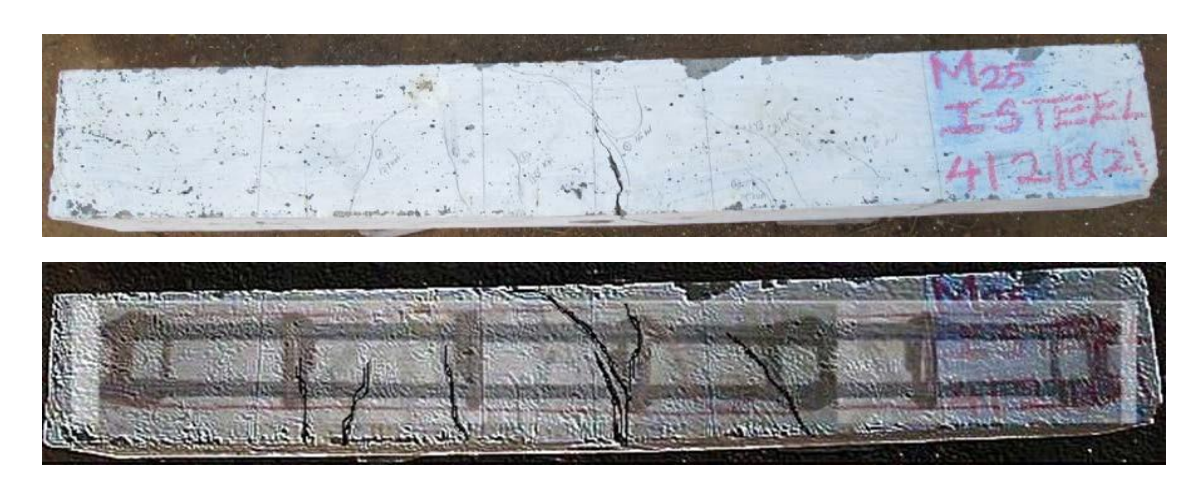


Fig. 33. Failure pattern of beams reinforced with diamond rib HYSD rebars.

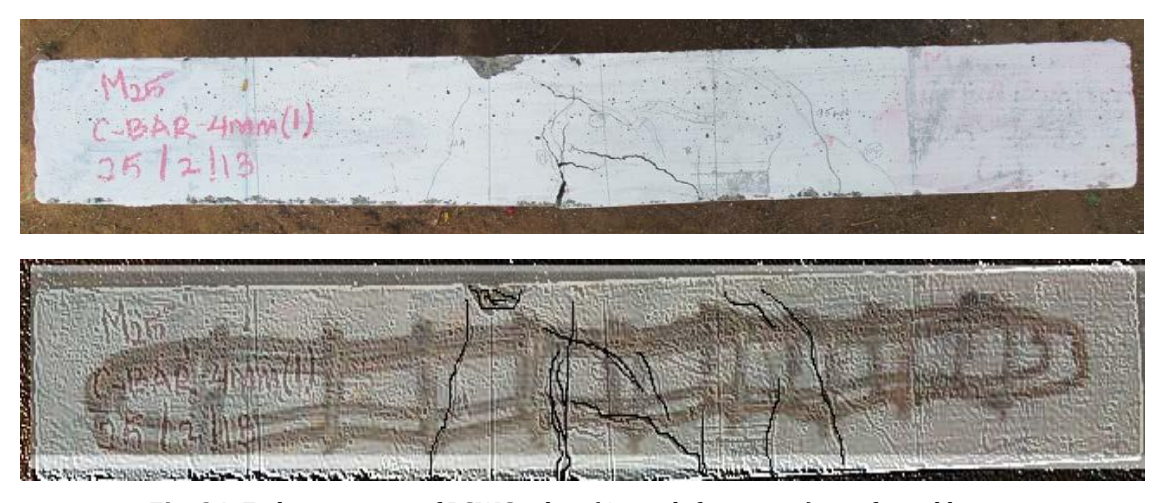


Fig. 34. Failure pattern of PSWC rebar (4mm deformation) reinforced beam.

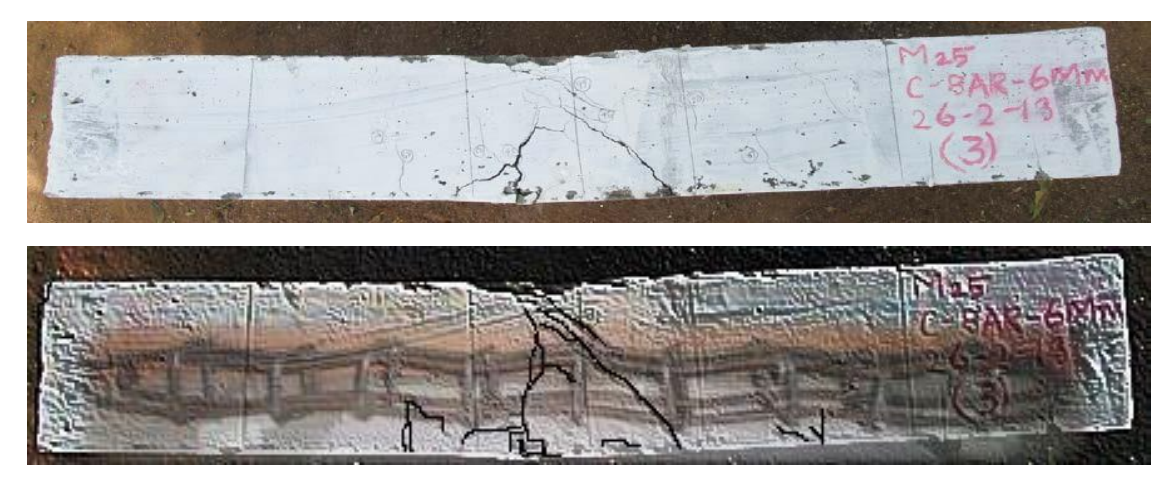
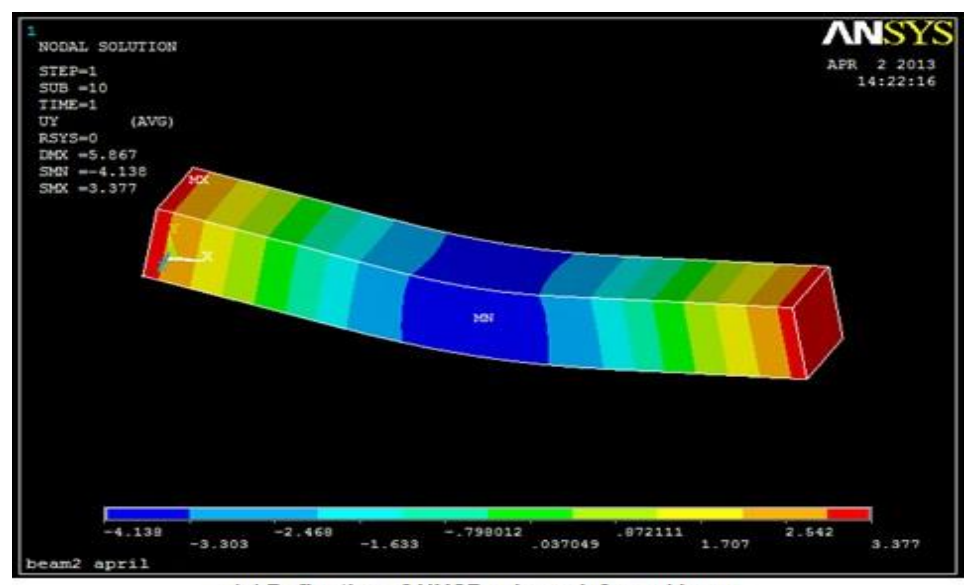
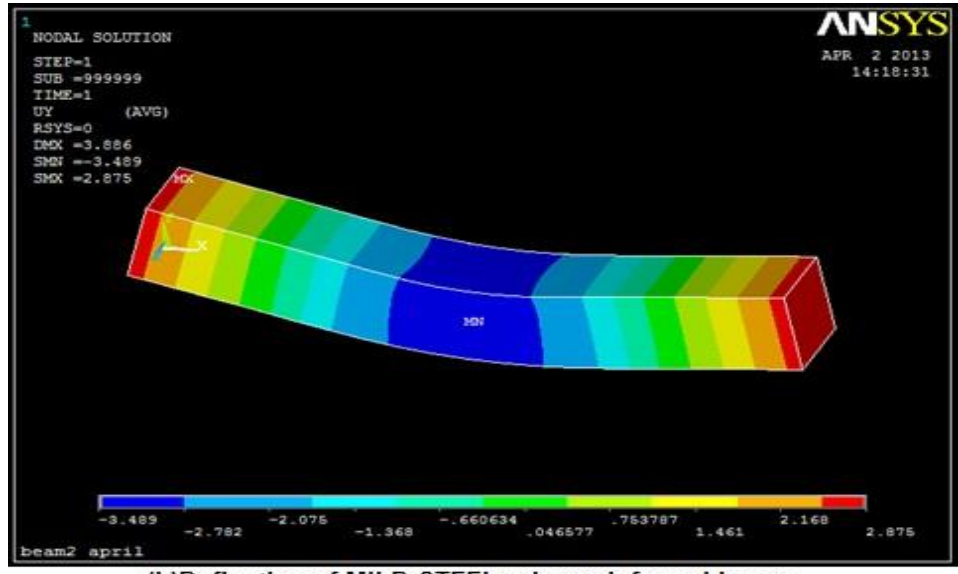


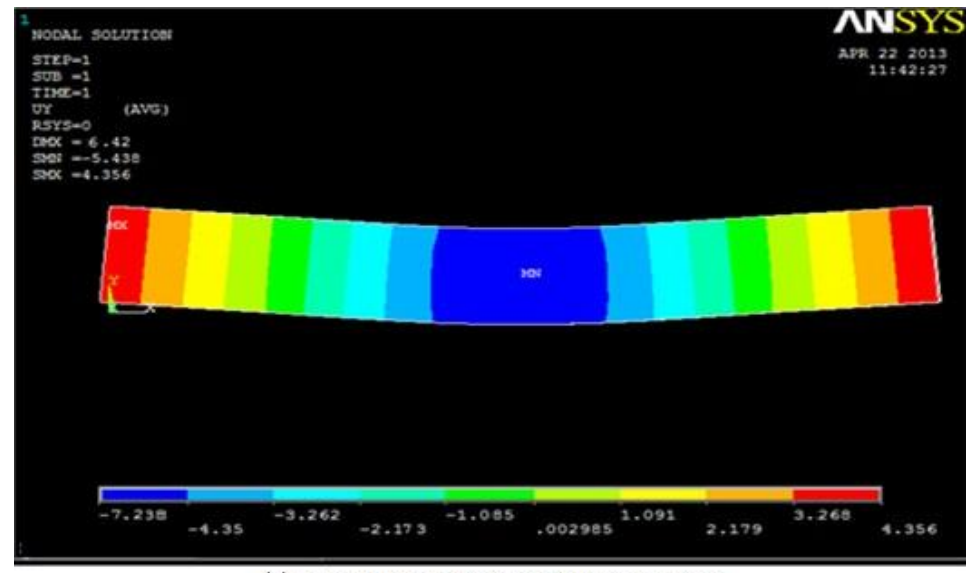
Fig. 35. Failure pattern of PSWC rebar (6mm deformation) reinforced beam.



(a) Deflection of HYSD rebar reinforced beam



(b)Deflection of MILD STEEL rebar reinforced beam



(c) Deflection of C-bar 6mm reinforced beam

Fig. 36. ANSYS deflection pattern for beams: (a) HYSD; (b) Mild steel; (c) PSWC rebars.

### 8. Conclusions

The test results obtained for PSWC rebar beams are interpreted and compared with HYSD and mild steel rebar beams and following conclusions are drawn:

- Incorporation of PSWC rebars as reinforcement in reinforced concrete beams has enhanced the ductile behaviour of the beams as compared to conventional HYSD and mild steel rebar beams.
- The energy absorbing capacity has increased significantly for beams reinforced with PSWC rebars when compared with conventional HYSD and mild steel rebar beams.
- The load-deflection behavior of PSWC rebar reinforced concrete beams was found to be similar to that of HYSD rebars irrespective of deformation level. The ultimate load carrying capacity of PSWC rebar reinforced beams is found to be less than that of HYSD rebar beams. This could be attributed to low compressive strength of concrete and yielding nature of PSWC rebar during the test.
- The failure mode of PSWC rebar reinforced concrete beams are found to be similar to that of HYSD rebar beams and crack width of PSWC bar reinforced beams are found to be smaller than HYSD rebar beams.
- The deflections of PSWC rebar reinforced beams were found to be higher than HYSD rebar beams which exhibits ductile behaviour of PSWC rebar reinforced heams
- The PSWC rebar beams offers good flexural performance enhancing the ductility and energy absorbing capacity irrespective of deformation levels.
- The analytical investigation from ANSYS gave good agreement with the experimental results.

It is concluded that PSWC rebar has the potential to replace conventional HYSD rebar. Further study needs to be done to optimize the profile level and stirrup locations; and usage with high concrete grade to get maximum benefit.

### REFERENCES

- Gagg CR (2014). Cement and concrete as an engineering material: an historic appraisal and case study analysis. Engineering Failure Analvsis, 40, 114-140.
- Garden HN, Quantrill RJ, Hollaway LC, Thorne AM, Parke GAR (1998). An experimental study of the anchorage length of carbon fibre composite plates used to strengthen reinforced concrete beams. *Construction and Building Materials*, 12(4), 203-219.
- Goyal A, Pouya HS, Ganjian E, Claisse P (2018). A review of corrosion and protection of steel in concrete. *Arabian Journal for Science and Engineering*, 43(10), 5035-5055.
- Hobbs DW (2001). Concrete deterioration: causes, diagnosis, and minimising risk. *International Materials Reviews*, 46(3), 117-144.
- IS:269 (1989). Specification for Ordinary Portland Cement. Bureau of Indian Standards, New Delhi, India.
- IS:516-1959 (2004). Indian Standard Methods for Test on Concrete. Bureau of Indian Standards, New Delhi, India.
- IS:2720 (1985). Methods of Tests for Soils, Part IV. Bureau of Indian Standards, New Delhi, India.
- IS:4031 (1989). Methods of Physical Tests for Hydraulic Cement. Part 6: Determination of Compressive Strength of Hydraulic Cement other than Masonry Cement. Bureau of Indian Standards, New Delhi, India
- IS:2386 (1963). Methods of Test for Aggregates for Concrete-Part 1: Particle Size and Shape. Bureau of Indian Standards, New Delhi, India.
- IS:10262 (2009). Concrete Mix Proportioning—Guidelines. Bureau of Indian Standards, New Delhi, India.
- Kar AK (2012). Durability of concrete bridges and viaducts. The Masterbuilder, 14(7), 110-130.
- Kar AK (2019). U.S. Patent Application No. 16/260,951.
- Marcos-Meson V, Michel A, Solgaard A, Fischer G, Edvardsen C, Skovhus TL (2018). Corrosion resistance of steel fibre reinforced concrete-a literature review. *Cement and Concrete Research*, 103, 1-20.
- Meddah MS, Bencheikh M (2009). Properties of concrete reinforced with different kinds of industrial waste fibre materials. *Construction and Building Materials*, 23(10), 3196-3205.
- Nanni A (2003). North American design guidelines for concrete reinforcement and strengthening using FRP: principles, applications and unresolved issues. *Construction and Building Materials*, 17(6-7), 439-446.
- Neville AM (1987). Why we have concrete durability problems. *Katherine and Bryant Mather International Conference on Concrete Durability*, American Concrete Institute, Detroit, ACI SP-100, 21-48.
- Song HW, Saraswathy V (2007). Corrosion monitoring of reinforced concrete structures – a review. *International Journal of Electrochemical Science*, 2, 1-28.
- Zhao Y, Yu J, Jin W (2011). Damage analysis and cracking model of reinforced concrete structures with rebar corrosion. *Corrosion Science*, 53(10), 3388-3397.



### Research Article

## Fracture patterns and mechanical properties of GFRP bars as internal reinforcement in concrete structures

Mehmet Canbaz a,\* D, Uğur Albayrak D

<sup>a</sup> Department of Civil Engineering, Eskişehir Osmangazi University, 26480 Eskişehir, Turkey

### **ABSTRACT**

Glass Fiber Reinforced Plastic (GFRP) composites as rolled bars can be used as steel rebar to prevent oxidation or rust which is one of the main reasons concrete structures deteriorate when exposed to chlorides and other harmful chemicals. GFRP is successful alternative for reinforcement with high tensile strength- low strain, corrosion resistance and congenital electromagnetic neutrality in terms of longer service life. The main goal of the study is to investigate the mechanical and bonding properties of GFRP bars and equivalent steel reinforcing bars then compare them. GFRP and steel rebar are embedded in concrete block with three different levels. Mechanical properties of GFRP and steel bars in terms of strength and strains are determined. On the other hand; modulus of elasticity of GFRP and steel bars, modulus of toughness and modulus of resilience were calculated using stress-strain curves, as a result of the experiments. Pull-out tests are conducted on each GFRP and rebar samples which are embedded in concrete for each embedment level and ultimate adherence strengths are determined in terms of bar diameter-development length ratio. Yield strength, strain and modulus of elasticities of GFRP samples are compared to steel rebar. According to the test results reported in this study, GFRP bars are used safely instead of steel bars in terms of mechanical properties.

### ARTICLE INFO

Article history:
Received 2 May 2020
Revised 3 June 2020
Accepted 17 June 2020

Keywords: GFRP bar Mechanical properties Pull-out test Steel reinforcing bar

### 1. Introduction

The behavior of glass fiber reinforced plastic (GFRP) bars as internal reinforcement for concrete structures has been investigated in a number of studies that GFRP reinforcement bars can increase the ductility, toughness and strength of structural members. Although GFRP bars are now commercially available, many civil engineers are not familiar with using GFRP rods as internal reinforcement for concrete structures which are especially in highly aggressive environment conditions. High tensile strength is one of the most important features of GFRP that the others are corrosion resistance, environmental stability, light weight and excellent bond strength (Gangarao et al., 2007). Fiber reinforced plastic (FRP) is made of a polymer matrix laminated with fibers which are widely glass or carbon and embedded in a resin matrix (Anurag et al., 2015; Agarwal et al., 2010). The most used FRP reinforcement types today; glass fiber reinforced plastic (GFRP), carbon fiber reinforced plastic (CFRP), aramid fiber reinforced plastic (AFRP), and basalt fiber reinforced plastic (BFRP) are the main known FRP reinforcements. The surface properties of these reinforcements can be changed by using different methods during the production phase. The most commonly used resin types in FRP reinforcement production as binders are thermoset polymer resins epoxies, polyester and vinyl esters. FRP rods are produced by pultrusion method. In this method, glass fibers are passed through the thermoset resin tank and smeared into the resin. Resin-impregnated glass fiber fibers enter the preform and allow the air and excess resin to be filtered in them. In addition, the penetration of the resin into the glass reinforcement material is achieved. Its surface is covered with mixed fiber fibers to protect it from the atmosphere and other external factors. Then the material that enters the main

<sup>\*</sup> Corresponding author. Tel.: +90-222-239-3750; Fax: +90-222-239-3613; E-mail address: mcanbaz@ogu.edu.tr (M. Canbaz) ISSN: 2548-0928 / DOI: https://doi.org/10.20528/cjcrl.2020.03.003

mold turns into a rod shape. The resin-fiber ratio plays a decisive role in the behavior of FRP within the structure. The most commonly used materials for structural applications are steel, aluminum and wood. However, in some applications these materials are gradually being replaced by glass fiber for reasons such as low specific weight and durability. FRP reinforcing bars are useful for R.C. structures where the existence of steel would not be applicable due to limited steel resources and good corrosion resistance of FRP composites (Bhashya et al., 2015; Vicki and Charles, 1993). Durability of FRP reinforcing concretes have been investigated mostly in recent years (Chen et al., 2007; Wang et al., 2007). On the other hand, bond behaviour between FRP and concrete is a one of the key factor to mitigate adhesion problems. Mechanical adherence or bond behaviour of the FRP bars to the concrete is proper as well as steel bars (Lawrence et al., 1998; Tepfers, 2006; Achillides and Pilakoutas, 2004). Creep resistance of glass FRP bars is quite good (Najafabadi et al., 2018). FRP can be used particularly in marine structures or in the evaluation of marine content such as coral aggregates in concrete production (Yang et al., 2018). Temperature increase significantly affects FRP thermal deformations (Zaidi et al., 2017). The deformation in FRP embedded concrete under high temperature was affected by fiber type (Aydın, 2018). After seawater immersion on the GFRP bars at a high temperature, micro cracks and voids appeared between the surface resin and fiber of the GFRP bars, and serious debonding and deterioration of glass fibers occurred (Wang et al., 2018). Bond properties between FRP bar and concrete is affected by various parameters like diameter of bar, sand coating etc. (Rolland et al., 2018; Albayrak and Canbaz, 2015). The use of GFRP in civil engineering applications is becoming increasingly common. In Fig. 1, it is seen that GFRP is used in many civil engineering applications, primarily in transportation and coastal structures (Durmaz, 2018).







Fig. 1. Application areas where GFRP is used.

Due to the brittle structure of GFRP, there has not been enough studies on its behavior in the structure. For this purpose, in this study, bonding behavior of steel and GFRP bars were investigated by pull-out tests, and mechanical properties of GFRP bars were investigated. Also crack patterns of GFRP under bending and tensile were examined.

### 2. Experimental Study

### 2.1. Materials

Cement: CEM I 42.5 cement was used by production of Çimsa Eskişehir cement mill. The properties of cement are given in Table 1.

GFRP: In the experimental work, 12 mm diameter glass FRP rebars supplied from Dost Ltd.Co. These rebars were obtained by laminating glass fiber with epoxy recipe in one direction. The properties are shown in Table 2.

Steel rebars: In this study, 12 mm diameter S420 type steel rebars provided from İzmir Demir Çelik Sanayi Inc.Co. was used. The properties are shown in Table 3.

Water: Eskişehir tap water was used. The chemical analysis of the drinkable water is given in Table 4.

Aggregate: In this study, the crushed sand produced by Selka Concrete Company and natural river sands that are derived from Sakarya River were used. Table 5 gives the properties of the aggregate. The granulometry of aggregate is shown in Fig. 2.

Table 1. Properties of cement.

Final setting time, min.	Density, g/cm <sup>3</sup>	Blaine, cm <sup>2</sup> /g	Strentgh, MPa	Expension, mm
260	3.17	3750	49.5	1.3

Table 2. Properties of GFRP.

Modulus of elasticity, GPa	Strain, %	Diameter, mm	Tensile str., MPa	Weight, g/m
40	2.8	12	1000	200

**Table 3.** Properties of steel reinforcing bars.

Tensile / Yield	Yield str., MPa	Strain, %	Modulus of elasticity, GPa	Poisson ratio
1.15	420	10	200	0.30

**Table 4.** Chemical analysis of the water.

рН	NTU	Cl mg/l	Ca++ mg/l	SO <sub>4</sub> mg/l	Organic Material	CO <sup>-3</sup> mg/l	FS0 mg/l	Mg++ mg/l	Total Salinity
7.7	<5	245.8	187	135	49	23	92	107,4	1540

**Table 5.** Properties of the aggregate.

Coarse	aggregate	Fine a	Water absorption,	
loose unit weight, kg/dm³ compact unit weight, kg/dm³		loose unit weight, kg/m <sup>3</sup>	compact unit weight, kg/m <sup>3</sup>	%
1.7	1.9	1,5	1,7	0.6

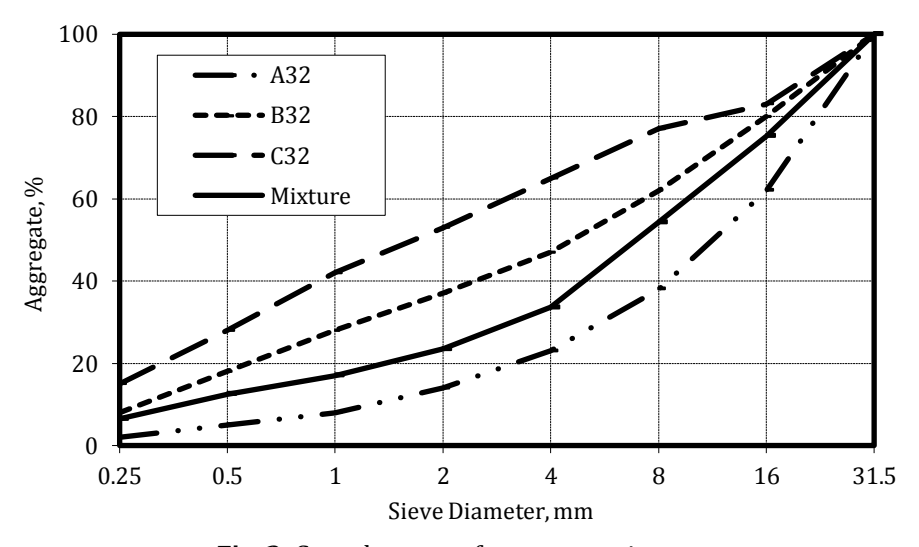


Fig. 2. Granulometry of aggregate mixture.

### 2.2. Method and tests

The purpose of this study is to investigate the bonding properties of FRP bars and compare them to that of steel reinforcing bars. In this preliminary experimental study, 12 mm diameter Glass FRP (GFRP) bars and 12 mm diameter S420 ribbed steel reinforcing bars were used. In the production of concrete basement, CEM I 42.5 type normal Portland cement and Eskişehir tap water were used.

Three types of aggregates (0–4, 4–8, and 8–32 mm) were used for adequate gradation of concrete mixtures. The solid concrete basement on the dimension 35x50x100 cm<sup>3</sup> by 0.5 water/cement ratio was produced. Composition of basement concrete was given in Table 6.

GFRP and steel bars were embedded perpendicular to the fresh concrete surface with quadrilateral meshing system. Concrete production, and rebar placement were shown in Fig. 3.



Fig. 3. Concrete production and rebar placement.

**Table 6.** Composition of concrete mixtures, kg/m<sup>3</sup>.

Cement	Water	0-4 mm, Crushed sand	4-8 mm, Crushed stone	8-32 mm, Crushed stone
300	150	900	700	400

The bars were embedded in concrete block with 3 different levels. Adherence (development) depth-diameter ratio (L/D) were considered 10, 15 and 20. Adherence strength of the bar specimens (Steel and GFRP) were determined by pull-out tests after 28 days shown in Fig. 4.



Fig. 4. Pull-out test.

Since concrete can be sufficient against the compressive strength, the tensile strength of FRP becomes important in strengthening. For this purpose, tensile and bending tests were conducted on reinforcing bars for determining the mechanical properties of FRP shown in Fig. 5.

### 3. Discussion

Bending tests with 90° and 135° angles were performed on 60 cm length GFRP samples and shown in Fig. 6. According to the bending test results; GFRP bars were ruptured after epoxy matrix phase and glass fibers were broken properly at inflection points. GFRP composites are not proper for bending because cannot make plastic deformations as a result of bending.



Fig. 5. Tensile tests conducted on reinforcing bars.

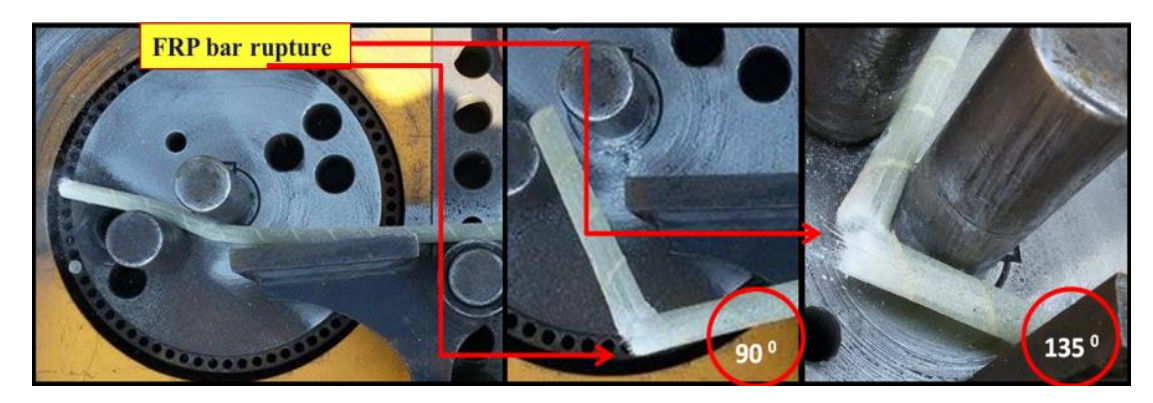


Fig. 6. Bending tests conducted on reinforcing bars.

As a result of the tension tests conducted on specimens, mechanical properties of the GFRP and Steel bars can be shown in Table 7. Tensile strength of GFRP bars are 93% of S420 steel bars approximately. On the other hand; modulus of elasticity of GFRP bars are less than 3.5 times to steel bars. Total elongation of GFRP bars are less than 5.5 times to steel bars while toughness of GFRP reinforcement was found to be about 15% of steel reinforcement.

Typical stress-strain curve for S420 and GFRP bars used in the study are shown in Fig. 7. In stress-strain curve for GFRP samples, the curve is linear until 150 MPa

stress level and fibers were not ruptured suddenly after the maximum stress point. The percentage elongation of all the samples tested was less than the minimum requirement of 10% for GFRP.

Rupture patterns of GFRP and steel bars after tensile tests are seen in Fig. 8. Expected progressive necking during tension test was not being observed in low carbon steel bars whereas 45° brittle failures were observing. GFRP bars with epoxy were ruptured into large pieces under ultimate stress longitudinally then fibers were appeared and the stress was reduced without completely rupturing.

	Yield Strength, MPa	Tensile Strength, MPa	Rupture Strength, MPa	Mod. of Elast., GPa	Elongation, mm	Reduction of Area %	Toughness Nmm/mm <sup>3</sup>
S420	512.82	618.92	565.87	123.52	20	30.56	116
GFRP		574.71		35.92	3.7		17

**Table 7.** Mechanical properties of the GFRP and steel bars.

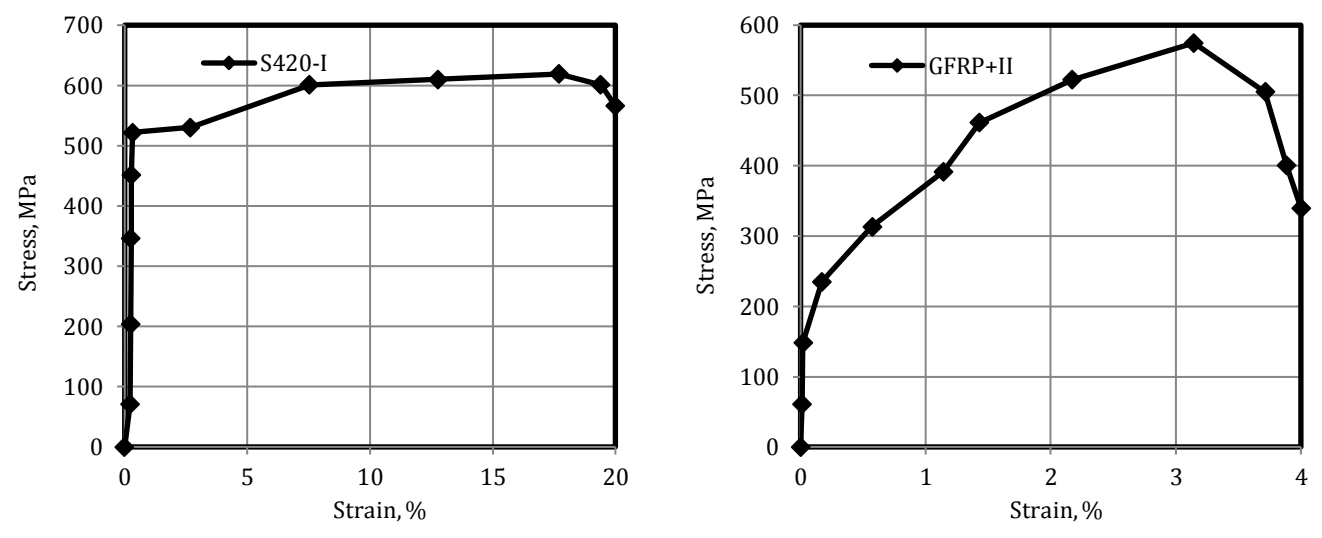


Fig. 7. Typical stress-strain curves for S420 and GFRP bars.



**Fig. 8.** Rupture patterns for S420 and GFRP bars.

Fiber type, resin type, surface properties, diameter, modulus of elasticity, embedment length, position of the reinforcement within the concrete, vertical and horizontal concrete cover, concrete strength, ratio of transverse reinforcement and the environmental conditions are the factors effecting the adherence of FRP (Basaran and Kalkan, 2020).

It can be expected that the adherence strengths of FRP reinforcements with concrete due to reasons such as the material properties of the FRP reinforcement are different and the production methods are different from the steel reinforcement-concrete adherence strength. Bonding

behavior of steel and GFRP bars were investigated by pull-out tests. Adherence strength values were determined based on bonding forces and the relationships between development depth and bar diameter were given in Fig. 9. Adherence strength increased as the development depth increased. Adherence strengths of steel and GFRP bars were increased up to 90% while the development length increased. Adherence strengths of GFRP bars are 85% of steel bars initially and decreased into 80% whereas the development length increased. GFRP bars have good adherence strength even though it is not ribbed.

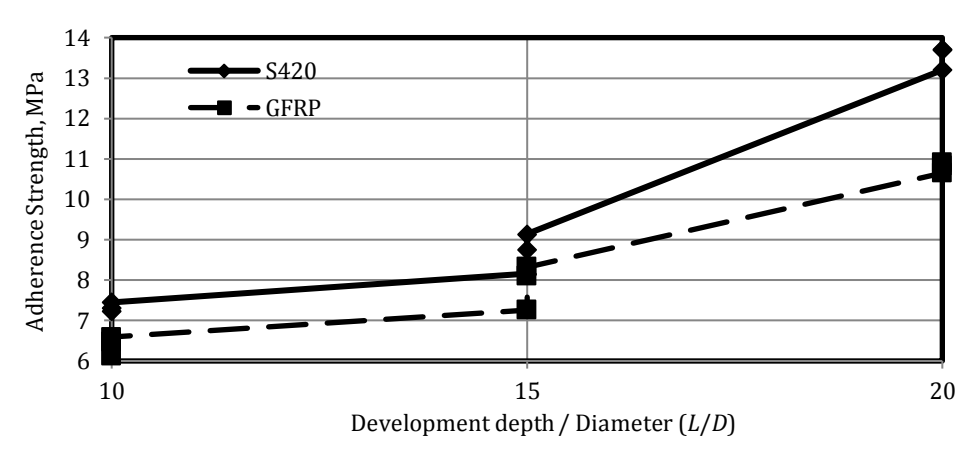


Fig. 9. Pull-out test results.

### 4. Conclusions

Preliminary test results that have been conducted on GFRP and steel bars indicate that:

- Deformation properties of GFRP reinforcements must be improved while tensile strengths of GFRP were enough in terms of mechanical behaviour. Using GFRP bars instead of steel bars in reinforced concrete members may lead to brittle failure. GFRP fibers were not completely ruptured after tension test while total strain values of GFRP bars are less than 5%. Yield strengths of steel bars were 125% of characteristic yield strength while tensile/yield ratio was 1.20. On the other hand, expected progressive necking on tension test was not being observed in steel bars. Brittle failure with 45° was observed in steel bar specimens.
- According to the pull-out tension test results; development length was increased also adherence strengths were increased. Adherence strengths of GFRP bars are 85% of steel bars initially and this ratio was decreased to 80% approximately when the development length increased. Adherence strengths of GFRP bars are adequate although there was no ribbed part on the GFRP surfaces.

It has been concluded that using GFRP bars instead of steel bars in reinforced concrete buildings and members may create undesirable results. GFRP bars are not proper for bending so cannot be used as tie or hooked bars. GFRP bars can be used credibly in reinforced concrete slabs or road pavements in order to solve corrosion problems. However, it is recommended to investigate its behavior under other chemical influences, such as acid. In addition, the pH of the concrete is very high. It is recommended to investigate the effect of this alkaline environment on GFRP in the long term.

### REFERENCES

Achillides Z, Pilakoutas K (2004). Bond behavior of fiber reinforced polymer bars under direct pullout conditions. *Journal of Composites for Construction*, 8(2), 173–181.

Agarwal A, Garg S, Rakesh PK, Singh I, Mishra BK (2010). Tensile behavior of glass fiber reinforced plastics subjected to different environmental conditions. *Indian Journal of Engineering and Materials Sciences*, 17, 471-476.

Albayrak U, Canbaz M (2015). Investigation of fiber reinforced plastic bars utilization instead of steel reinforcing bars in terms of mechanical properties. 2nd International Conference on Computational and Experimental Science and Engineering – ICCESEN, 1(1), 264.

Anurag G, Singh H, Walia RS (2015). Effect of fillers on tensile strength of pultruded glass fiber reinforced polymer composite. *Indian Journal of Engineering and Materials Sciences*, 22, 62-70.

Aydin F (2018). Experimental investigation of thermal expansion and concrete strength effects on FRP bars behavior embedded in concrete. *Construction and Building Materials*, 163, 1-8.

Basaran B, Kalkan I (2020). Investigation on variables affecting bond strength between FRP reinforcing bar and concrete by modified hinged beam tests. *Composite Structures*, 112185.

Bhashya V, Kumar SS, Ramesh G, Bharatkumar BH, Krishnamoorthy TS, Nagesh RI (2015). Long term studies on FRP strengthened concrete specimens. *Indian Journal of Engineering and Materials Sciences*, 22, 465-472.

Chen Y, Davalos JF, Raya I, Kim HY (2007). Accelerated aging tests for evaluations of durability performance of FRP reinforcing bars for concrete structures. *Composite Structures*, 78, 101–111.

Durmaz N (2018). Investigation of flexural behaviour of FRP reinforced concrete slabs. *M.Sc. thesis*, Sakarya University, Sakarya, Turkey.

Gangarao HVS, Taly N, Vijay PV (2007). Reinforced Concrete Design with FRP Composites. CRC Press, Taylor & Francis Group, Florida, USA.

Lawrence CB, Puterman M, Katz A (1998). The effect of material degradation on bond properties of fiber reinforced plastic reinforcing bars in concrete. *Materials Journal*, 95, 232-243.

Najafabadi EP, Bazli M, Ashrafi H, Oskouei AV (2018). Effect of applied stress and bar characteristics on the short-term creep behavior of FRP bars. *Construction and Building Materials*, 171, 960-968.

Rolland A, Quiertant M, Khadour A, Chataigner S, Benzarti K, Argoul P (2018). Experimental investigations on the bond behavior between concrete and FRP reinforcing bars. *Construction and Building Materials*, 173, 136-148.

Tepfers R (2006). Bond clause proposals for FRP bars/rods in concrete based on CEB/FIP Model Code 90. Part 1: Design bond stress for FRP reinforcing bars. *Structural Concrete*, 7, 47-55.

Vicki LB, Charles LB (1993). FRP reinforcing bars in reinforced concrete members. *Materials Journal*, 90-1, 34-39.

Wang L, Mao Y, Lv H, Chen S, Li W (2018). Bond properties between FRP bars and coral concrete under seawater conditions at 30, 60, and 80°C. Construction and Building Materials, 162, 442-449.

Wang YC, Wong PMH, Kodur V (2007). An experimental study of the mechanical properties of fibre reinforced polymer (FRP) and steel reinforcing bars at elevated temperatures. *Composite Structures*, 80, 131-140.

Yang S, Yang C, Huang M, Liu Y, Jiang J, Fan G (2018). Study on bond performance between FRP bars and seawater coral aggregate concrete. Construction and Building Materials, 173, 272-288.

Zaidi A, Brahim MM, Mouattah K, Masmoudi R (2017). FRP properties effect on numerical deformations in FRP bars-reinforced concrete elements in hot zone. *Energy Procedia*, 139, 798-803.



### Research Article

# Comparative study of optimum cost design of reinforced concrete retaining wall via metaheuristics

Aylin Ece Kayabekir <sup>a</sup> 🕞, Melda Yücel <sup>a</sup> 🕞, Gebrail Bekdaş <sup>a</sup> 🕞, Sinan Melih Nigdeli <sup>a,\*</sup> 🕞

### **ABSTRACT**

Design engineers may find various options of metaheuristic method in optimization of their problems. Because of the randomization nature of metaheuristic methods, solutions may trap to non-optimum solutions which are just optimums in a limited part of the selected range of the design variables. Generally, metaheuristics use several options to prevent this situation, but the same optimization process may solve different performances in every run of the process. Due to that, a comparative study by using ten different algorithms was done in this study. The optimization problem is the cost minimization of an L-shaped reinforced concrete (RC) retaining wall. The evaluation is done by conducting 30 multiple cycles of optimization, and comparing minimum cost, average cost and standard deviation values.

### ARTICLE INFO

Article history: Received 8 June 2020 Revised 4 July 2020 Accepted 16 July 2020

Keywords:
Metaheuristic
Optimization
Reinforced concrete retaining wall
Structural optimization
Robustness

### 1. Introduction

Metaheuristic methods are iterative methods, which are generally used for optimizing mathematical and engineering problems including constraints. Due to constraints, the nature of the problems is non-linear, and metaheuristics can easily handle these problems. A metaheuristic method has several formulations to reach the optimum value. These formulations may be given for different types of generation of new variables with random values within the solution range. Also, the formulations of metaheuristics have several inspirations using a metaphor. The metaphors are listed in Table 1. The details about special features of algorithms can be seen in the cited papers given in Table 1.

Reinforced concrete (RC) structures are consisting of two materials, and these materials have different costs, strength and mechanical behaviour. For that reason, the optimum cost design problem is highly constrained by structural state limits such as stress capacities, ductile behaviour requirements, minimum and maximum reinforcements.

In the design of structures, the stress on critical sections must be provided according to the internal forces such as flexural moment, axial force and shear forces. The ductile behaviour of structures are provided by considering several rules defined in the design codes. The basic rule for the members under flexural moment is the limitation of the reinforcement bars to provide the yielding of rebar before the fracture of the concrete. Due to this reason, the stress limitations cannot be directly considered as single material structures. In that case, the balance between the stress of concrete in the compressive section of the member and the stress of rebar in tensile section must be investigates as seen in Fig. 1. The symbols of Fig. 1 are defined in Table 1.

If the maximum reinforcement is not enough for the design flexural moments, doubly reinforced design can be employed. In the wall type structures and retaining walls, doubly reinforced design is not preferred in practice. In that case, the reinforcements are limitated with singly reinforced design, and calculation is done for the unit meter of wall by taking  $b_w$  as 1m. Additionally, stirrups are not provided to carry shear forces in the RC retaining walls.

In addition to the structural state limits, RC retaining walls also contains geotechnical state limit. The geotechnical limit states are checked to provide stability of retaining walls. These controls include overturning, sliding and bearing capacity of the wall according to forces of self-weight, stresses under the footing, surcharge load and soil loads.

<sup>&</sup>lt;sup>a</sup> Department of Civil Engineering, İstanbul University-Cerrahpaşa, 34320 İstanbul, Turkey

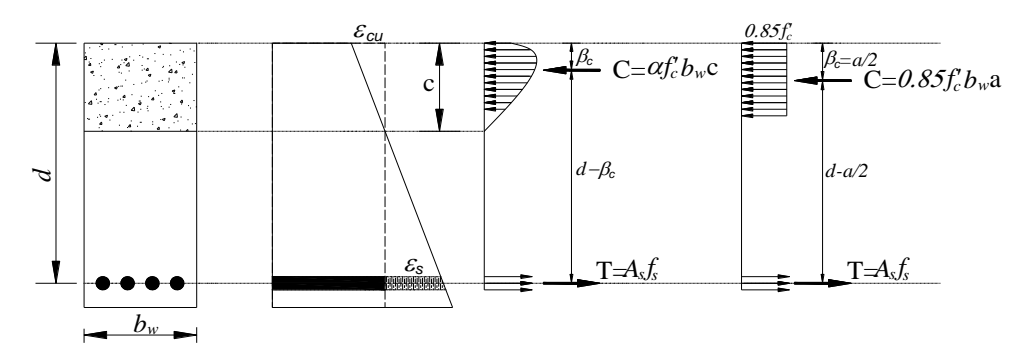


Fig. 1. A RC cross-section under flexure (Kayabekir et al., 2020).

Table 1. Notation of RC section with stress.

Symbol	Definition
$b_w$	web width, or diameter of circular section
d	$\ distance\ from\ extreme\ compression\ fiber\ to\ centroid\ of\ longitudinal\ tension\ reinforcement$
С	distance from extreme compression fiber to neutral axis
$eta_c$	distance from centroid of compressive stress block to face of compressive section
$f_c'$	specified compressive strength of concrete
$f_s$	calculated tensile stress in reinforcement at service loads
$A_s$	area of nonprestressed longitudinal tension reinforcement

Due to that, the optimum design of RC retaining walls have been solved via several metaheuristic methods including Genetic Algorithm (Kaveh et al., 2013), Particle Swarm Optimization (Ahmadi-Nedushan and Varaee, 2009), Big Bang-Big Crunch (Camp and Akin, 2012), Harmony Search (Kaveh and Abadi, 2011), Firefly Algorithm (Sheikholeslami et al., 2014), Simulated Annealing (Ceranic et al., 2001), Charged System Search (Yepes et al., 2008), Biogeography-based optimization (Aydogdu,

2017), Flower Pollination Algorithm (Mergos and Mantoglou, 2019), Gravitational Search Algorithm (Khajehzadeh et al., 2013).

In the present study, the optimization of L-shaped retaining walls was done by using 10 different algorithms given in Table 2. Optimum results were compared by conducting 30 multiple cycles of optimization of design data. The evaluation is presented according to minimum, average cost and standard deviation of 30 independent runs.

Table 2. Metaphor used in metaheuristic.

Algorithm	Metaphor	Citation
Genetic algorithm (GA)	Natural selection	Holland (1974)
Differential Evolution (DE)	Natural selection	Storn and Price (1997)
Particle Swarm Optimization (PSO)	Behaviours of colonies	Kennedy and Eberhart (1995)
Harmony Search (HS)	Musical performance of musician	Geem et al. (2001)
Artificial Bee Colony Algorithm (ABC)	Natural behaviours of bee colonies as food-searching	Karaboğa (2005)
Firefly Algorithm (FA)	Flashing ability of firefly	Yang (2009)
Teaching-Learning-Based Optimization (TLBO)	Principle of teach to students by a teacher and self-learn by them in a class	Rao et al. (2011)
Grey Wolf Optimization (GWO)	Conception of leadership hierarchy with hunting behaviour in nature belonging grey wolfs	Mirjalili et al. (2014)
Flower Pollination Algorithm (FPA)	Flowering process of plant's	Yang (2012)
Jaya Algorithm (JA)	Victory	Rao (2016)

### 2. Design Methodology

The algorithms used in the study are chosen from classical algorithms, proved algorithms with their success on engineering problems and recent algorithms. The most known classical algorithms such as GA, DE and

PSO are chosen. The proved algorithms used in the comparative study are HS, ABC and FA. The recent ones are FPA, GWO and parameter-free algorithms such as TLBO and JA. JA also contain a single phase of optimization, and it is the most basic one to apply on an engineering problem.

The design steps are summarized in the flowchart given as Fig. 2. This flowchart is a general one for metaheuristic algorithms.

In the methodology, the design constants (constant parameters of RC retaining wall), ranges of design variables, algorithm specific parameters, population number and a maximum iteration number are defined. Then, an initial solution matrix containing sets of candidate design variables is generated within the selected range of design variables. The number of sets of design variables is equal to the population. Then, the analysis of the RC retaining wall is done, and the total material cost of the wall is calculated for all set of design variables. The cost is saved since it is the objective function tried to minimize. If one of the design constraints is not provided, the cost is penalized with a huge value. After the generation of the initial solution matrix, the iteration process starts. The solution matrix is updated by using special features of the algorithms, and the updated solutions are saved instead of previous ones if the cost is smaller than the cost value

of the previous ones. The iterations of updating the solution matrix continue for maximum number of iterations.

### 3. RC Retaining Wall Example and Optimum Results

The figure of the retaining wall is shown in Fig. 3. The design variables are listed in Table 3 including limit values of the range of optimization. The problem has 4 design variables and it have 16 design constraints given in Table 4. The first 4 of the design constraints are about the geotechnical state limit. The other ones are related to structural state limits. These limits are considered according to ACI318: Building Code Requirements for Structural Concrete (2014). The design constants and coefficients used in the study are given as Table 5.

The optimum results are provided by the usage of 20 populations and 5000 iterations and applying as 30 cycles. The results are presented in Tables 6-8 for walls with H=3m, 7m and 10m, respectively.

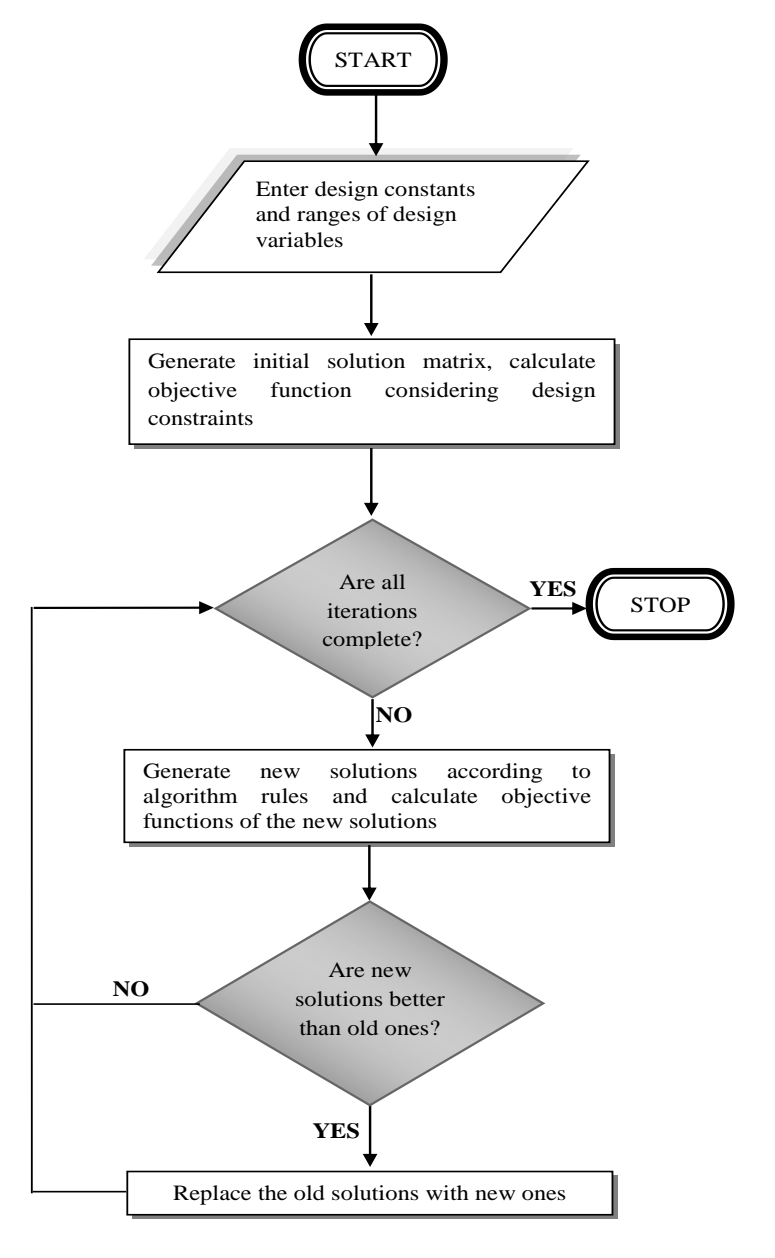


Fig. 2. General flowchart of optimization process.

 Table 3. The design variables and ranges.

Definition	Symbol	Limit/Value	Unit
Heel slab/back encasement width of retaining wall	$X_1$	0-10	m
Upper part width of cantilever/stem of wall	$X_2$	0.2-3	m
Bottom part width of cantilever/stem of wall	$X_3$	0.3-3	m
Thickness of bottom slab of retaining wall	$X_4$	0.3-3	m

**Table 4.** The design constraints.

Description	Constraints
Safety for overturning stability	$g_1(X)$ : $FoS_{ot,design} \ge FoS_{ot}$
Safety for sliding	$g_2(X)$ : $FoS_{s,design} \ge FoS_s$
Safety for bearing capacity	$g_3(X)$ : $FoS_{bc,design} \ge FoS_{bc}$
Minimum bearing stress ( $q_{min}$ )	$g_4(X)$ : $q_{min} \ge 0$
Flexural strength capacities of critical sections $(M_d)$	$g_{5-7}(X): M_d \ge M_u$
Shear strength capacities of critical sections $(V_d)$	$g_{8-10}(X): V_d \ge V_u$
Minimum reinforcement areas of critical sections ( $A_{smin}$ )	$g_{11-13}(X): A_s \ge A_{smin}$
Maximum reinforcement areas of critical sections ( $A_{smax}$ )	$g_{14-16}(X): A_s \le A_{smax}$

**Table 5.** The design constants.

Definition	Symbol	Value	Unit
Difference between top elevation of bottom-slab with soil in behind of wall (active zone)/stem height	Н	3-7-10	m
Weight per unit of volume of back soil of wall (active zone)	$\gamma_{\rm z}$	18	kN/m³
Surcharge load in active zone (on top elevation of soil)	$\mathbf{q}_{\mathrm{a}}$	10	kN/m <sup>2</sup>
Angle of internal friction of back soil of wall	Φ	30°	-
Allowable bearing value of soil	qsafety	300	kN/m <sup>2</sup>
Thickness of granular backfill	$t_b$	0.5	m
Maximum Coefficient of soil reaction	$K_{soil}$	200	MN
Compressive strength of concrete	$f_c$	25	MPa
Tensile strength of steel reinforcement	fy	420	MPa
Elasticity modulus of concrete	$E_s$	200000	MPa
Weight per unit of volume for concrete	$\gamma_{c}$	25	kN/m³
Weight per unit of volume for steel	$\gamma_s$	7.85	t/m³
Width of wall bottom slab	В	1000	mm
Concrete unit cost	$C_{\rm c}$	50	\$/m <sup>3</sup>
Steel unit cost	$C_{\rm s}$	700	\$/ton
Coefficient for load increment	$C_1$	1.7	-
Reduction coefficient for section bending moment capacity	FiM	0.9	-
Reduction coefficient for section axial load capacity	FiN	0.9	-
Reduction coefficient for section shear load capacity	FiV	0.75	-
Constant load coefficient	$G_{\mathrm{K}}$	0.9	-
Live load coefficient	$Q_{\rm K}$	1.6	-
Horizontal load coefficient	$H_{\text{K}}$	1.6	-

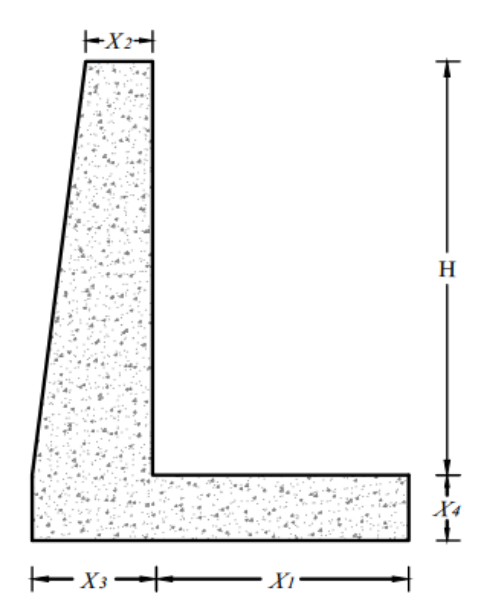


Fig. 3. The L-shaped design retaining wall.

**Table 6.** The optimum results (H=3 m).

Algorithm	$X_1$	X <sub>2</sub>	X <sub>3</sub>	$X_4$	Min. Cost	Ave. Cost	Standard Dev.
GA	2.2229	0.2002	0.3016	0.3004	108.68944	114.84902	15.98500
DE	2.2234	0.2000	0.3000	0.3000	108.58173	116.65465	34.03933
PSO	2.2234	0.2000	0.3000	0.3000	108.58173	108.58173	0.00000
HS	2.2234	0.2000	0.3000	0.3000	108.58246	108.59081	0.00801
FA	2.2234	0.2000	0.3000	0.3000	108.58173	108.58178	0.00004
ABC	2.2236	0.2000	0.3000	0.3000	108.58564	109.03591	0.78806
TLBO	2.2234	0.2000	0.3000	0.3000	108.58173	108.58173	0.00000
FPA	2.2234	0.2000	0.3000	0.3000	108.58173	108.58173	0.00000
GWO	2.2234	0.2000	0.3000	0.3000	108.58173	110.14573	2.65610
JA	2.2234	0.2000	0.3000	0.3000	108.58173	108.58173	0.00000

**Table 7.** The optimum results (H=7 m).

Algorithm	$X_1$	X <sub>2</sub>	X <sub>3</sub>	X <sub>4</sub>	Min. Cost	Ave. Cost	Standard Dev.
GA	4.7632	0.2005	0.7533	0.5275	605.01168	621.63784	35.41998
DE	4.7608	0.2000	0.7493	0.5150	604.75489	614.48449	38.08353
PSO	4.7610	0.2000	0.7492	0.5152	604.75519	654.04851	122.48324
HS	4.7693	0.2000	0.7425	0.5242	604.85495	605.35279	0.32382
FA	4.7598	0.2000	0.7505	0.5143	604.75832	604.79833	0.02365
ABC	4.7616	0.2001	0.7473	0.5116	604.85052	606.95079	3.92429
TLBO	4.7608	0.2000	0.7492	0.5150	604.75489	604.75489	0.00000
FPA	4.7608	0.2000	0.7493	0.5150	604.75489	604.76417	0.03294
GWO	4.8056	0.2000	0.6763	0.4991	606.83137	621.57701	11.35595
JA	4.7609	0.2000	0.7492	0.5150	604.75489	604.75489	0.00000

Algorithm	$X_1$	X <sub>2</sub>	X <sub>3</sub>	X <sub>4</sub>	Min. Cost	Ave. Cost	Standard Dev.
GA	6.8824	0.2007	1.6700	0.7535	1469.46405	1500.24786	21.94036
DE	6.7810	0.2000	1.6843	0.7202	1467.19368	1558.93810	175.31755
PSO	6.7788	0.2000	1.6841	0.7190	1467.20136	167998.77360	372082.280
HS	6.7759	0.2000	1.6803	0.7144	1467.40149	1468.68387	0.66989
FA	6.7904	0.2000	1.6834	0.7236	1467.25477	101320.66730	299559.777
ABC	6.7924	0.2000	1.6802	0.7220	1467.30247	1469.01494	2.10107
TLBO	6.7809	0.2000	1.6843	0.7201	1467.19369	1467.19380	0.00014
FPA	6.7810	0.2000	1.6843	0.7202	1467.19368	1467.27857	0.28631
GWO	7.0103	0.2082	1.6741	0.7993	1481.74107	1504.86350	15.40662
JA	6.7810	0.2000	1.6843	0.7202	1467.19368	1520.97722	53.46521

**Table 8.** The optimum results (H=10 m).

### 4. Conclusions

In this study, an optimization application was performed intended for weight minimization of an L-shape retaining wall to detect the best design algorithm providing the required constraints and conditions. In this regard, all processes were applied by using thirty cycles, and statistical calculations were made according to mean and standard deviation results given in Tables 6-8 for 3m, 7m and 10m, respectively.

According to the results, it can be recognized that the minimum weight of 3m L-shape retaining wall is 108.58173 and this was reached via 7 algorithms from 10. On the other hand, two of these algorithms are not effective in means of mean and deviation values. These algorithms are GWO and especially DE. PSO, TLBO, FPA and JA are very successful due to the least deviation as zero. FA can be considered an effective method to find the best results due to its error value is slightly much from them.

It can be seen that for H=7 m, which is the second model used for wall height, the best weight value (604.75489) was obtained with DE, TLBO, FPA and JA. TLBO and JA achieved this by making without a deviation. Although DE achieved to this, standard deviation value of weight function is very big cause that weight is so different and far from minimum weight in every cycle. Additionally, also FPA, which has an error that it is pretty close of both methods, can be preferred for determination of minimum weight.

Finally, if the 10m retaining wall is evaluated, it can be seen that again DE, FPA and JA are effective methods in finding the best value. But, the most successful one is FPA, because it did not make big deviations. DE and even JA extremely deviated while reaching the minimum weight. In this case, this shows that both methods find very different results for weight in every cycle. Also, TLBO is effective to find a result which is slightly different than the optimum result with small deviation.

When these three wall models were evaluated, noticed that successful algorithm number decreases as long as increasing of wall height. Also, DE is not steady in

terms of to find the minimum weight in every cycle of optimization with regards to all wall heights. To sum up, FPA and TLBO are the most convenient algorithms, which can be preferred among whole metaheuristics thanks to that it succeeds in terms of achievement for providing of desired results for all heights.

### REFERENCES

ACI 318-14 (2014). Building Code Requirements for Structural Concrete and Commentary. ACI Committee. Farmington Hills, MI.

Ahmadi-Nedushan B, Varaee H (2009). Optimal design of reinforced concrete retaining walls using a swarm intelligence technique. *Proceedings of the first International Conference on Soft Computing Technology in Civil, Structural and Environmental Engineering*, UK.

Aydogdu I (2017). Cost optimization of reinforced concrete cantilever retaining walls under seismic loading using a biogeography-based optimization algorithm with Levy flights. *Engineering Optimization*, 49(3), 381-400.

Camp CV, Akin A (2012). Design of retaining walls using big bang-big crunch optimization. *Journal of Structural Engineering*, 138(3), 438-448.

Ceranic B, Fryer C, Baines RW (2001). An application of simulated annealing to the optimum design of reinforced concrete retaining structures. *Computers & Structures*, 79(17), 1569-1581.

Geem ZW, Kim JH, Loganathan GV (2001). A new heuristic optimization algorithm: harmony search. *Simulation*, 76(2), 60-68.

Holland JH (1975). Adaptation in natural and artificial systems, University of Michigan Press. Ann Arbor, MI.

Karaboga D (2005). An idea based on honey bee swarm for numerical optimization. Technical Report TR06, (Vol. 200, pp. 1-10), Department of Computer Engineering, Engineering Faculty, Erciyes University, Turkey.

Kaveh A, Abadi ASM (2011). Harmony search based algorithms for the optimum cost design of reinforced concrete cantilever retaining walls, *International Journal of Civil Engineering*. 9(1) 1-8.

Kaveh A, Kalateh-Ahani M, Fahimi-Farzam M (2013). Constructability optimal design of reinforced concrete retaining walls using a multiobjective genetic algorithm. Structural Engineering and Mechanics, 47(2), 227-245.

Kayabekir AE, Bekdaş G, Nigdeli SM (2020). Metaheuristic Approaches for Optimum Design of Reinforced Concrete Structures: Emerging Research and Opportunities: Emerging Research and Opportunities. IGI Global. USA

- Kennedy J, Eberhart RC (1995). Particle swarm optimization. Proceedings of IEEE International Conference on Neural Networks No. IV, Perth Australia; November 27 - December 1. 1942–1948
- Khajehzadeh M, Taha MR, Eslami M (2013). Efficient gravitational search algorithm for optimum design of retaining walls. Structural Engineering and Mechanics, 45(1), 111-127.
- Mergos PE, Mantoglou F (2020). Optimum design of reinforced concrete retaining walls with the flower pollination algorithm. *Structural and Multidisciplinary Optimization*, 61(2), 575-585.
- Mirjalili S, Mirjalili SM, Lewis A (2014). Grey wolf optimizer. *Advances in Engineering Software*, 69, 46-61.
- Rao RV, Savsani VJ, Vakharia DP (2011). Teaching-learning-based optimization: a novel method for constrained mechanical design optimization problems. *Computer-Aided Design*, 43(3), 303-315.
- Rao R (2016). Jaya: A simple and new optimization algorithm for solving constrained and unconstrained optimization problems. *Interna*tional Journal of Industrial Engineering Computations, 7(1), 19-34.

- Sheikholeslami R, Khalili BG, Zahrai SM (2014). Optimum cost design of reinforced concrete retaining walls using hybrid firefly algorithm. *International Journal of Engineering and Technology*, 6(6), 465.
- Storn R, Price K (1997). Differential evolution—a simple and efficient heuristic for global optimization over continuous spaces. *Journal of global optimization*, 11(4), 341-359.
- Yang XS (2009). Firefly algorithms for multimodal optimization. In Stochastic algorithms: foundations and applications, Springer, Berlin Heidelberg, 169-178.
- Yang XS (2012). Flower pollination algorithm for global optimization. International Conference on Unconventional Computing and Natural Computation, September Heidelberg-Berlin, Springer, 240-249.
- Yepes V, Alcala J, Perea C, González-Vidosa F (2008). A parametric study of optimum earth-retaining walls by simulated annealing. *Engineering Structures*, 30(3), 821-830.